Alexandria Engineering Journal 94 (2024) 131–148

Contents lists available at ScienceDirect

Alexandria Engineering Journal

journal homepage: www.elsevier.com/locate/aej

Original article

Energy and economic analysis of building integrated photovoltaic thermal system: Seasonal dynamic modeling assisted with machine learning-aided method and multi-objective genetic optimization

Bashar Shboul [a], Mohamed E. Zayed [b,*], Waqar Muhammad Ashraf [c], Muhammad Usman [d], Dibyendu Roy [e], Kashif Irshad [b], Shafiqur Rehman [b]

[a] Renewable Energy Engineering Department, Faculty of Engineering, Al Al-Bayt University, Mafraq, Jordan
[b] Interdisciplinary Research Center for Sustainable Energy Systems (IRC-SES), King Fahd University of Petroleum & Minerals, Dhahran, 31261, Saudi Arabia
[c] The Sargent Centre for Process Systems Engineering, Department of Chemical Engineering, University College London, Torrington Place, London WC1E 7JE, UK
[d] Department of Mechanical Engineering, University of Engineering and Technology, Lahore, Pakistan
[e] Department of Engineering, Durham University, Durham, DH1 3LE, UK

ARTICLE INFO

Keywords:
Building integrated photovoltaic thermal system
Cost effective technology
Multi-objective performance optimization
Sensitivity analysis
Artificial intelligence

ABSTRACT

Building integrated photovoltaic thermal (BIPV/T) systems offer a highly effective means of generating clean energy for both electricity and heating purposes in residential buildings. Hence, this article introduces a new BIPV/T system to optimally minimize the energy consumption of a household residential building. The meticulous design of the proposed BIPV/T system is accomplished through MATLAB/Simulink® dynamic modeling. Performance analysis for the BIPV/T system is performed under different seasonal conditions with in-depth techno-economic analyses to estimate the expected enhancement in the thermal, electrical, and economic performance of the system. Moreover, a sensitivity analysis is conducted to explore the impact of various factors on the energetic and economic performances of the proposed BIPV/T system. More so, the two-layer feed-forward back-propagation artificial neural network modeling is developed to accurately predict the hourly solar radiation and ambient temperature for the BIPV/T. Additionally, a multi-objective optimization using the NSGA-II method is also conducted for the minimization of the total BIPV/T plant area and maximization of the total efficiency and net thermal power of the system as well as to estimate the optimized operating conditions for input variables across different seasons within the provided ranges. The sensitivity analysis revealed that higher solar flux levels lead to increased electric output power of the BIPV/T plant, but total efficiency decreases due to higher thermal losses. Moreover, the proposed NSGA-II shows a feasible method to attain a maximum net thermal power and optimal total efficiency of 5320 W and 63% with a minimal total plant area of 32.89 m^2 that attained a very low deviation index from the ideal solution. The levelised cost of electricity is obtained as 0.10 $/kWh under the optimal conditions. Thus, these findings offer valuable insights into the potential of BIPV/T systems as a sustainable and efficient energy solution for residential applications.

1. Introduction

Energy needs worldwide experienced a 2.1% rise in 2017, surpassing the previous year's growth rate and propelled by strong global economic progress. This increase was driven by the utilization of oil, gas, and coal. Consequently, there was a 1.4% increase in global CO_2 emissions during the same period [1]. Therefore, there has been a rapid upsurge in energy generation, leading to significant environmental concerns, including the occurrence of abnormal climate variations such as the melting of snow caps, global warming, drought, desertification, hurricanes, tsunamis, and more [2], [3].

Efficiently substituting fossil fuel sources, which contribute significantly to global warming, with eco-friendly energy resources poses a considerable obstacle in achieving energy sustainability, ensuring a reliable power supply, and addressing pressing environmental concerns [4]. Consequently, the emergence of the concept of renewable energy has gained substantial attention from prominent research institutions, economic experts, and, notably, stakeholders who stand to gain from the

* Corresponding author.
E-mail address: mohamed.zayed@kfupm.edu.sa (M.E. Zayed).

https://doi.org/10.1016/j.aej.2024.03.049
Received 7 October 2023; Received in revised form 28 January 2024; Accepted 18 March 2024
Available online 26 March 2024

widespread adoption of renewable energy technologies worldwide [5].

Governments are presently being urged to give careful consideration to renewable energy sources as replacements for conventional energy sources due to various concerns, with global warming being a significant factor that continues to escalate. Addressing the detrimental effects of conventional power sources should be their primary focus [6], [7]. The buildings sector currently accounts for approximately 36% of global energy consumption, resulting in nearly 40% of all carbon dioxide emissions. Moreover, buildings consume over 55% of the world's electricity, which exhibits an annual growth rate of 2.5% [8]. An optimal solution lies in transforming buildings into self-sufficient energy producers by harnessing renewable energy resources such as solar energy, wind energy, bioenergy, and geothermal energy, among others [9].

Solar thermal energy stands out as one of the most promising forms of renewable energy. These technologies facilitate the conversion of solar energy into heat, which can be utilized directly or further converted into electricity, enabling its application in any manner similar to conventional electricity [10]. The utilization of solar thermal energy offers several advantages, such as a virtually limitless energy supply, substantial cost savings with up to a 60% reduction in water heating energy and a 35% reduction in space heating energy, compatibility with existing systems, and the effectiveness of modern solar thermal systems [11]. Consequently, there has been a growing interest in both photovoltaic (PV) and thermal systems for various terrestrial applications, including extensive research and development of hybrid or integrated thermal/electric plate collectors, particularly for building applications [12], [13].

BIPV/T systems represent a renewable energy solution that integrates thermal collectors and PV panels into a unified module. The underlying concept of BIPV/T systems revolves around harnessing solar energy to generate both heat and power for buildings. [14]. BIPV/T systems hold significant potential as a primary urban renewable energy source, serving various purposes [15]. This technology integrates solar PV modules and solar thermal elements with building structures, including window design, roof systems, facades, and awnings, customized to meet the specific requirements of buildings [16], [17]. The functioning of a BIPV/T system involves an absorber comprised of an array of solar cells generating electricity, while a collector fluid passes through the absorber, extracting thermal energy, similar to a conventional flat plate collector [18]. The primary purpose of this technology is to enhance the efficiency of PV cells by cooling them, utilizing the absorbed heat from the sun's radiation [19]. Consequently, BIPV/T systems hold economic and practical appeal for a wide range of applications, including residential and non-residential buildings such as homes, hospitals, and various other structures [20]. Furthermore, BIPV/T systems can be employed to cater to additional energy requirements like lighting, heating, and cooling, expanding their versatility and potential applications. They outperform separate thermal and PV systems, generating more energy per unit area [21]. Additionally, innovative designs can enhance user interaction and promote widespread adoption of these systems in well-designed buildings [22]. By combining heating and energy production, BIPV/T systems require less space compared to separate systems [23]. Moreover, their implementation leads to a reduction in the social cost of carbon, resulting in environmental benefits and improved public health [24]. Furthermore, BIPV/T systems contribute to reduced utility and maintenance expenses, offering potential cost savings [25].

Several studies have been encompassed to investigate the performance and feasibility of building-integrated photovoltaic/thermal (BIPV/T) systems. Koondhar et al. [26] systematically conducted comparative analyses on various parameters of PV modules by employing an equivalent circuit diagram of moderate complexity. The simulation of the PV model enables the exploration and analysis of the relationships between V-I and P-V across varying temperatures and insolation levels for PV modules. Yang et al. [27] conducted simulations using TRNSYS tool to analyze the impact of design parameters on building performance, emphasizing the importance of the solar heat gain coefficient and thermal transmittance of BIPV/T windows. Chen et al. [28] focused on sub-tropical cities and simulated a case study to determine optimal parameters for PV/T-based solar trigeneration systems. Their results indicated the privileges of combining cryogenic energy storage and glazed PV/T collectors. Shoaib and Amin [29] explored the competitiveness of an air-based BIPV/T system with heat recovery using a thermal wheel, presenting enhanced thermal performance compared to independent BIPV/T configurations. Shahsavar et al. [30] carried out a comparative assessment between hybrid BIPV/T and ground-coupled air heat exchanger systems, revealing the upgraded effectiveness of the hybrid system. Investigations also highlighted the potential of renovating BIPV/T systems in the Canadian residential sector [31]. The assimilation of phase change materials (PCMs) in BIPV/T systems was analyzed, demonstrating improved thermal stability and electrical production [32]. The optimization of PV/T facades was assessed, confirming the significance of considering both electrical and thermal performance, as well as energy efficiency and wind resistance [33]. Moreover, examinations were executed on particular system types, such as a BIPV/T system for a high-rise building in Naples, Italy, demonstrating the advantages in terms of energy savings and economic gains [34]. Heat pipe-based PV/T systems have been studied, indicating the impact of design parameters on heat transfer and total system performance [35]. The comprehensive analysis of a heat pipe PV/T system highlighted its potential for high energy efficiency and reduced greenhouse gas emissions [36]. Sohani et al. [37] evaluated a hybrid solar-powered system combining rooftop photovoltaic PV and BIPV/T systems. The system reduces the load on the heating and air conditioning unit while generating electricity, resulting in at least 50% more electricity generation and a 60% reduction in heating and cooling loads. The system demonstrates a payback time of 2.87 years and sensitivity analysis reveals the influence of thermal comfort setpoints, inflation, and discount rates on system performance metrics. Abdalgadir et al. [38] a numerical study has investigated a coupled BIPV system associated with air handling unit using MATLAB/Simulink®, aiming to reduce winter heating demand and prevent high PV cell temperatures in summer. The results showed promising potential, with reduced heating loads and improved electrical power output through PV cell cooling.

Presently, machine learning models (ANN), have also garnered significant attention from researchers studying various configurations of BIPV systems. Fu et al. [39] employed the support vector machine (SVM) method for forecasting the overall exergy yield of a combined 100% renewables system, incorporating a BIPV/T system and an earth air heat exchanger. The statistical evaluation of the SVM performance revealed a substantial accuracy level, with an R value of 0.9670, in modeling the annual exergy. Zazoum [40] employed Gaussian process regression (GPR) with SVM approaches for predicting the power output of a PV system, conducting a comparative analysis. The findings indicated that, between the two approaches, GPR exhibited superior performance, with RMSE and R^2 values of and 7.976 and 0.9802, respectively. Khandakar et al. [41] applied ANN alongside the M5P decision tree, and linear regression techniques for predicting the power output of a PV/T system. The findings indicated that ANN yielded significantly lower errors, specifically a root mean square error of 2.1436. Lee et al. [42] constructed a data-driven modeling employing an ANN for the estimation of the maximum power point (MPP) in a BIPV/T system. The validation results of the model demonstrated its effective performance in estimating the MPP for the BIPV/T system, showcasing a CvRMSE of under 30%. Tien et al. [43] provided a synopsis of recent progress in utilizing machine learning methods to improve building energy efficiency. The literature indicated successful applications of machine learning in building energy efficiency, the majority of studies remain in the experimental or testing phase. Furthermore, there is a scarcity of research that has implemented machine learning strategies in real-world buildings and conducted post-occupancy evaluations.

1.1. Literature discussion and research gaps identification

Overall, the above-summerized studies contribute to the understanding of BIPV/T systems, their design parameters, performance optimization, and potential applications in various contexts. They provide valuable insights for researchers and practitioners aiming to implement sustainable and efficient energy solutions in buildings. Overall, BIPV/T systems represent an efficient and sustainable approach to integrating thermal and PV technologies for renewable energy generation. The majority of existing research papers have predominantly focused on investigating other established renewable energy systems such as PV, BIPV, and solar thermal collectors for residential applications. However, BIPV/T systems face certain obstacles, including high initial costs, which potentially render them more expensive and less competitive compared to separate PV and solar thermal systems [37]. When dealing with large installation areas, it may be more effective to opt for distinct PV and solar thermal systems. Nevertheless, the above-mentioned survey encountered several challenges primarily due to the limited availability of previous research on BIPV/T systems. In this context, several research gaps can be identified based on the literature as critically given:

1. Existing research primarily concentrates on other renewable energy systems, neglecting the specific investigation of BIPV/T systems. There is a need for more comprehensive analysis and research specifically addressing BIPV/T systems.
2. The high initial costs associated with BIPV/T systems hinder their competitiveness compared to separate PV and solar thermal systems. Further investigation is necessary to explore the economic viability, cost-benefit analysis, and potential cost-reduction strategies for BIPV/T systems.
3. Although certain aspects of BIPV/T systems have been explored, more research is required regarding integration strategies, optimization techniques, and design guidelines. This includes optimizing system layouts and exploring further design parameters to enhance the overall performance of BIPV/T systems.
4. Modeling the performance measures of BIPV/T by artificial neural networks is also missing in the literature.

1.2. Contribution and novelty of the research

Hence, this study aims to address the mentioned existing research gaps by proposing an economically efficient design solution and artificial intelligent based techno-economic-energetic optimization of an improved BIPV/T design framework. The paper conducts a comprehensive and systematic numerical investigation into dynamic modeling, sensitivity analysis, and performance optimization for the proposed BIPV/T system under several seasonal conditions. The meticulous design of the proposed BIPV/T system is accomplished through MATLAB/Simulink® dynamic modeling. The key objectives and novelties of this research can be delineated as follows:

1. Multi-objective optimization was performed to establish the most favorable operational and design parameters, considering the minimization of the total BIPV/T plant area and maximization of the total efficiency and net thermal power of the system. The examined system underwent optimization through a hybrid method, combining artificial intelligence with the Non-dominated Sorting Genetic Algorithm II (NSGA-II) and integrating the Technique for Order of Preference by Similarity to Ideal Solution (TOPSIS).
2. A detailed performance analysis for the BIPV/T system is performed under different seasonal conditions of Mafraq, Jordan with in-depth techno-economic analyses to estimate the expected enhancement in the thermal, electrical, and economic performance of the system.
3. Sensitivity analysis is also conducted to explore the impact of irradiance, wind speed, and inlet air temperature to assess the electrical and thermal efficiency of the system under varying conditions.

The present results anticipated that the suggested framework stands as a valuable guide for shaping the design of BIPV/T projects, fostering the creation of solutions that are both efficient and cost-effective. This has the potential to encourage the widespread incorporation of BIPV/T in building projects under varying meteorological conditions in different continental regions.

2. Methods

This research paper evaluates the techno-economic performance of BIPV/T configuration for residential usage in Mafraq City, Jordan. To achieve that, this investigation calculates various parameters, such as the estimated temperature of the panels before and after cooling, the electrical and thermal efficiencies, the thermal electrical power production, and the plant size and area for a typical household.

The data used for the analysis was obtained from a selected household in Mafraq in which the energy consumption is considered average. The data were analyzed to provide an estimation of the system's performance and its impact on efficiency. This study aimed to examine the energy consumption of a domestic household based on the BIPV/T power production in order to observe the improvement of the system's power generation while requiring a smaller installation area than other alternative systems in the fields.

2.1. Meteorological data and site selection

The significance of meteorological data and choosing an appropriate site for a project in Mafraq city is of utmost importance. The research work outcomes can be greatly influenced by the weather, terrain, and infrastructure. Analyzing BIPV/T systems requires careful consideration of meteorological data and site selection, as these factors play a critical role in determining the effectiveness and viability of such systems.

Mafraq city is positioned in the northern-central part of Jordan (32.2°N, 36.84°E) and is characterized by a hot and arid climate [44]. The average yearly temperature stands at 20 °C [45], with the peak months of June and July reaching an average of 28 °C. Conversely, the coldest months of January and February see temperatures averaging around 7 °C [45]. Given that BIPV/T module installation requires extensive land usage and demands unobstructed areas, Mafraq City's topography proves advantageous for such energy systems. Jordan, situated in the MENA region, stands out as an ideal location for the establishment of BIPV/T plants. With an estimated average direct normal irradiance (DNI) of 2700 kWh/m^2 and an impressive count of approximately 300 clear and sunny days per year, totaling 3311 hours, the country boasts one of the most favorable environments for such installations [46]. Specifically, Mafraq, with a daily average DNI ranging from 6.54 to 7.29 kWh/m^2 and an annual average wind speed of 4.72 m/s, enjoys plentiful solar irradiation and abundant wind resources, as shown in Fig. 1. Furthermore, a study conducted by Shboul et al. [47] supports the notion that Mafraq is among the most suitable regions in Jordan for harnessing solar energy potential and implementing solar thermal technology plants. Consequently, the city of Mafraq has been chosen as the primary location for the case study, aimed at investigating the performance of BIPV/T systems within the context of this research endeavor. The benefits offered by BIPV/T systems surpass any potential disadvantages, establishing them as a sensible investment for both businesses and homeowners in the city.

2.2. ANN meteorological data prediction model

This section aims to present the capability of the developed meteorological forecasting model using state-of-the-art ANN techniques to

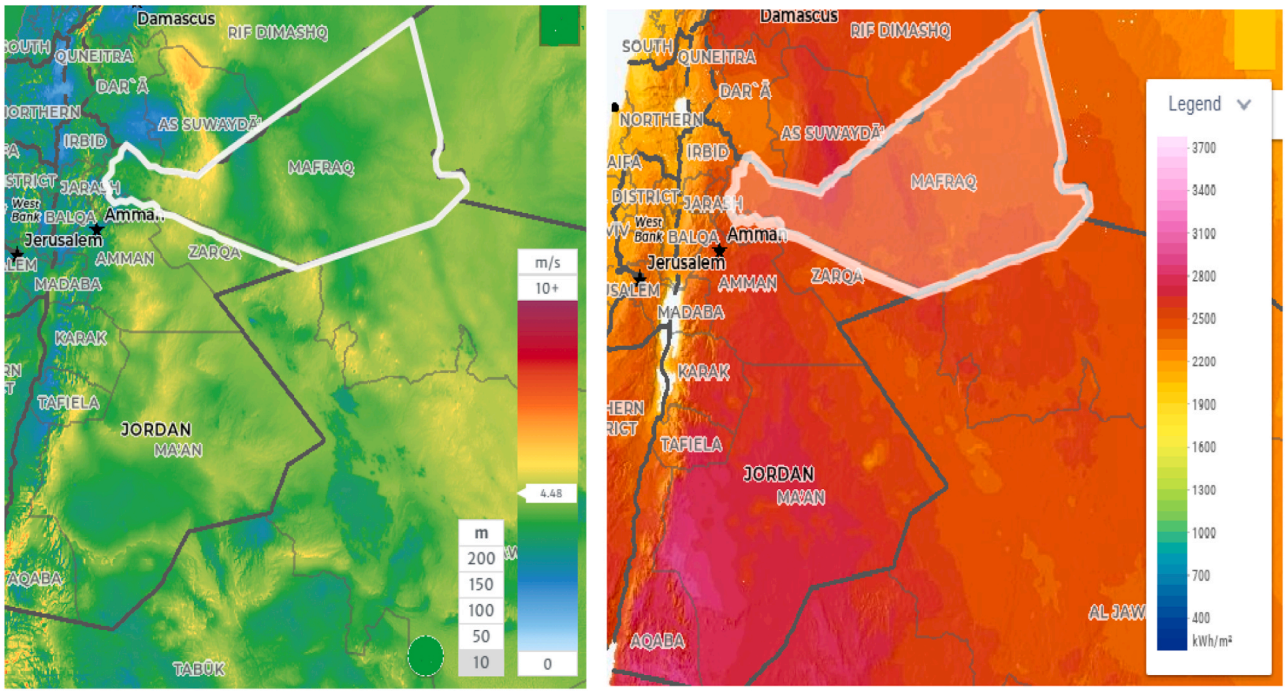

Fig. 1. The distribution of wind speed and solar DNI in Mafraq, Jordan.

predict the hourly solar radiation and ambient temperature data for the selected location in Mafraq, Jordan across all seasons throughout the year.

The data-driven ANN model is selected in this study due to its several advantages over the first-principle-based mechanistic model: the simulation and prediction are fast and computationally cheap, and the model-based multi-objective optimization analysis is more computationally efficient than the mechanistic model-based analysis which can be computationally prohibitive [48]. Thus, the comprehensive ANN-based modeling and optimization approach can help policymakers and energy practitioners to analyze in reasonable domain time and with good accuracy thereby accelerating the design and performance enhancement-based analyses and tasks. Another advantage of using ANN algorithm for the modelling tasks is its ability to mine the nonlinear patterns and relationships amongst the variables and effectively approximating the nonlinear function space [48]. The ANN algorithm requires less computational resources and a few hyperparameters tuning in comparison with other machine learning algorithms like support vector machine and random forest algorithm which is a remarkable feature of the algorithm [48].

In this context, these two essential meteorological parameters are assigned as inputs to simulate the BIPV/T unit in the adopted location by the MATLAB/Simulink® software. A newly ANN forecasting model is developed based on Solargis™ measured data [42], to obtain highly accurate predictions (error less than 3%) for solar radiation and ambient temperature over 20 years in Mafraq, Jordan. Noteworthy, it is acknowledged that the current analysis employs the same approach and methodology by using the validated data as input parameters within the MATLAB/Simulink® software in this study. Despite that, a slight modification was made to the inputs and outputs of the previously developed ANN model to match the target of the present work. The study utilizes the two-layer feed-forward back-propagation artificial neural network (2 L-FFBPANN) model developed using MATLAB/Simulink®. The model aims to accurately predict hourly solar radiation and ambient temperature by correlating historical meteorological data over the proposed BIPV/T system in Mafraq, Jordan. The output layer of the 2 L-FFBPANN consists of four neurons representing global horizontal irradiation (GHI), DNI, diffuse horizontal irradiance (DHI), and ambient temperature (T_a). Input indices include the day of the month, the month of the year, and clock time, while meteorological variables such as cloud identification quality, sun azimuth and altitude angles, wind speed and direction, humidity, pressure, and precipitation are used. As a result, the 2 L-FFBPANN model serves as a reliable tool for forecasting solar and temperature indices. The model aims to achieve a close match between the predicted output and the desired targets, represented by a slope of 45° indicating perfect fitting. Training stops immediately when the validation error no longer changes. Fig. 2 illustrates high accuracy values exceeding 0.97 are attained for the predicated solar irradiation during training, validation, testing, and overall dataset. It is evident that the 2 L-FFBPANN model accurately predicts meteorological parameters in close agreement with measured ones.

The accuracy of the forecasting model is illustrated in Fig. 3, indicating the MAPE trends for the targeted outputs, namely GHI and weather temperature over an entire year. The adopted location exhibits an exceptional model performance, with an average MAPE below 6.78% and consistently low MAPE values below 0.4% throughout the year, demonstrating remarkable accuracy. Fig. 3(a) highlights the MAPE for GHI in Mafraq, denoting consistently low errors below 7% for the majority of the year in the studied area. Fig. 3(b) displays the MAPE for ambient temperature readings, with the error percentage rarely exceeding 3% at any given time, indicating a high level of precision.

A custom MATLAB/Simulink® signal builder has been developed to generate 1-hour-based input parameters for the 2 L-FFBPANN model, allowing for the evaluation of hourly variations in GHI and T_a throughout the year at the selected location. After that, the resulting output of the BIPV/T configuration is analyzed for each hour over a year, as depicted in Fig. 4 for the winter season specifically, revealing the dynamic variations. Each hour is represented as a 1-second signal within the signal builder block, refer to Fig. (4). As a result, Fig. 4(b) and Fig. 4 (c) present the hourly profiles of GHI (W/m^2) and T_a (°C) in Mafraq, illustrating their patterns throughout the year and the four seasons, respectively. The 1-hour timescale provides insights into the variations of GHI and T_a, capturing the maximum and minimum values.

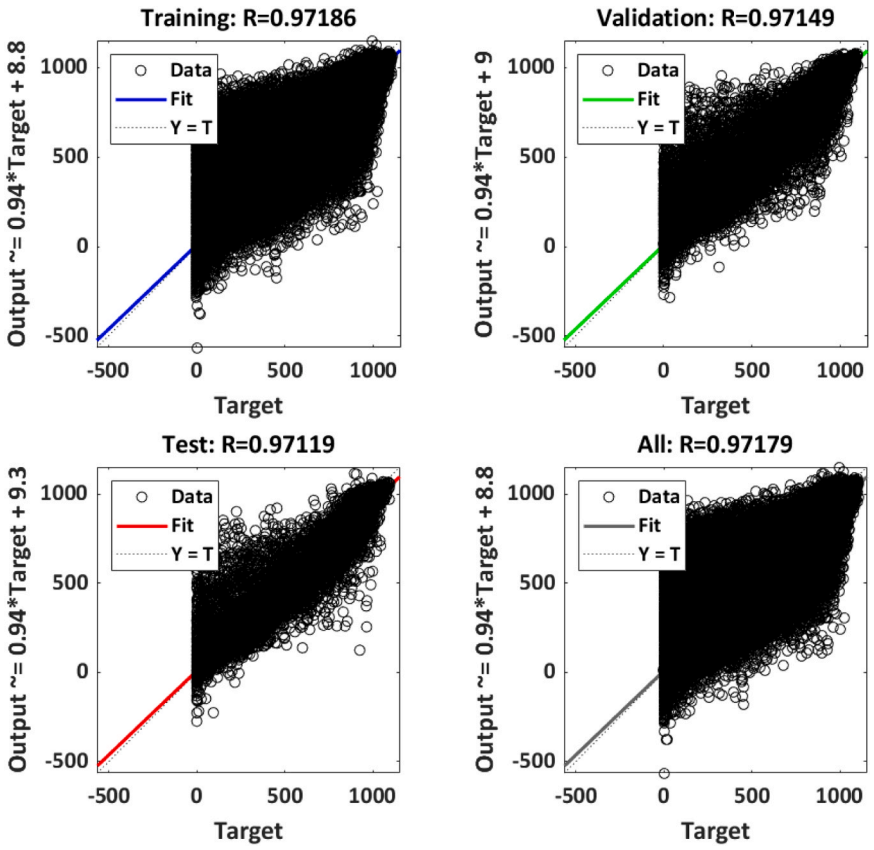

Fig. 2. Regression plot of the predicted GHI and ambient temperature obtained by the 2 L-FFBPANN model during training, validation, and testing stages.

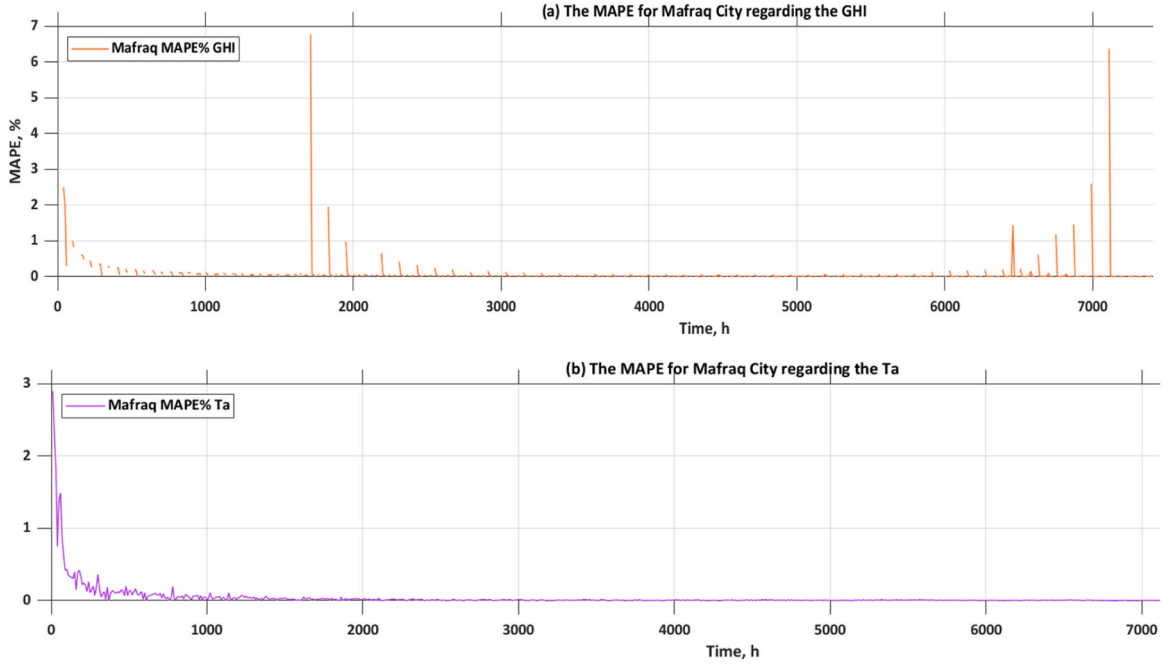

Fig. 3. The MAPE of climatic conditions for Mafraq City regarding, (a) GHI and (b) Ambient temperature.

2.3. Simulation model and design data

In this empirical investigation, the simulation model and design data employed are outlined in this section. The model creation took place using MATLAB/Simulink®, utilizing mathematical equations that define the behavior of the integrated BIPV/T module. The specific data concerning electricity and water consumption was gathered from a residential building located in Mafraq, Jordan.

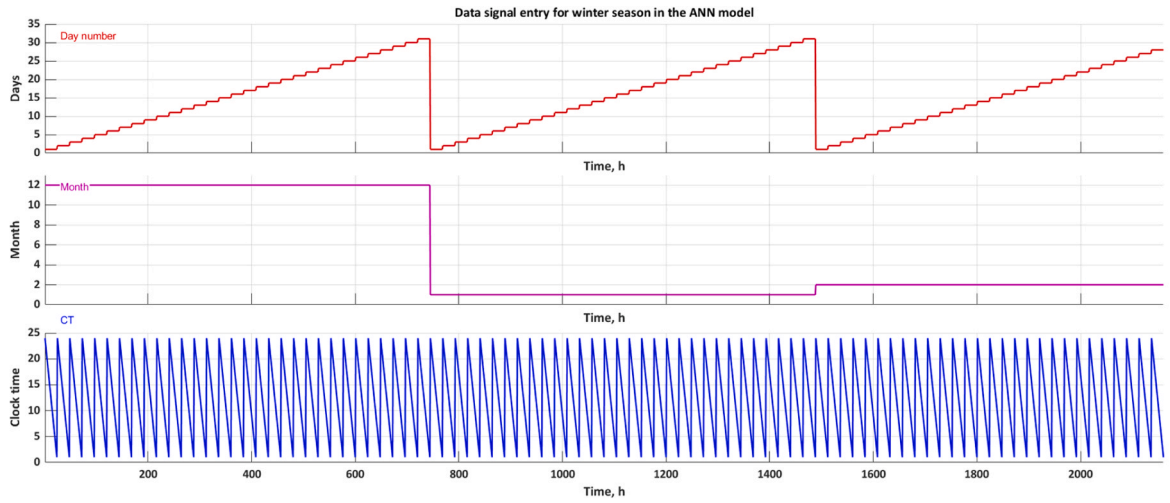

(a). Time-based data signal entry for the winter season in the FFBPANN model.

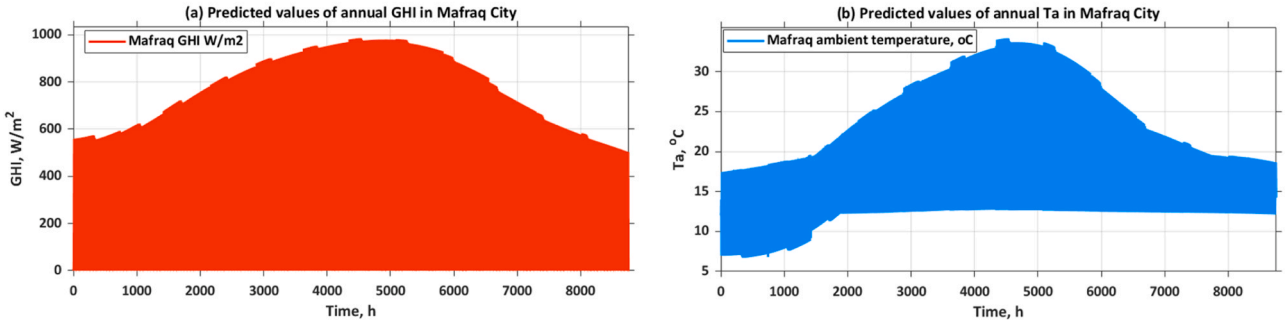

(b). Hourly profile along the year for GHI and ambient temperature for Mafraq, Jordan.

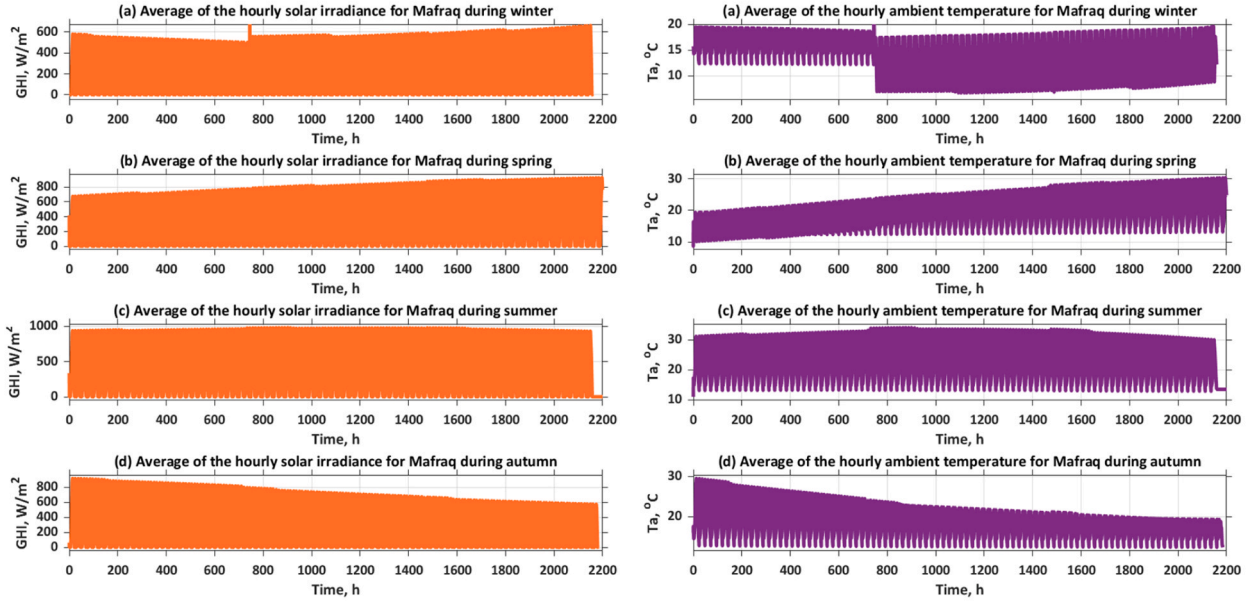

(c). Prdicted hourly profiles along the year seasons for GHI and ambient temperature for Mafraq city, Jordan.

Fig. 4. (a). Time-based data signal entry for the winter season in the FFBPANN model.

2.3.1. *Simulation model*

MATLAB/Simulink® is a versatile software application widely used for designing renewable energy systems. It has been specifically adapted for the BIPV/T modeling and rigorous simulation appraisal due to its exceptional capabilities in developing regulation algorithms. The utilization of rigorous software like MATLAB/Simulink® allows designers to easily develop new models or updates to previously established ones. This powerful tool provides a user-friendly graphical interface (GUI), where the models could be established as block diagrams operating with simple click-and-drag mouse actions. With the user-friendly interface, individuals can build models in a way that resembles a hands-on approach to sketching with pen and paper.

A robust modeling software has been developed using the MATLAB/Simulink® software, integrating collected meteorological data obtained

from the Solargis™. The BIPV/T model parameters are carefully interrelated, ensuring robust integration. Notably, all mathematical model equations are solved simultaneously, distinguishing it from other software that solves subsystems autonomously. Moreover, the system runs through an iterative loop solution, enabling a bidirectional flow of data across the whole system. The current model is established based on a design technique, employing the calculation and measurement of system design, size, and cost. Users can assign inlet system parameters, and MATLAB/Simulink® display blocks readily present the calculated design data, including size, energy, and cost. The user-friendly model is shown in Fig. 5.

2.3.2. Data description

The proposed residential building is situated in a sun-drenched region with an average annual solar irradiance for Global Horizontal Irradiance (GHI) at the site varies in the range of 500–986 W/m^2. The dwelling possesses a roof area spanning 200 m^2, indicating the available space suitable for the installation of solar panels or other applications. The hot water requirement comprises a monthly volume of 10 m^3 and an annual consumption of 120 m^3. These specifications facilitate an evaluation of the potential for solar energy generation on the roof, as well as insights into the capacity necessary to fulfill the monthly and yearly hot water demands. This assessment includes considerations for system size and storage capacity. The limitations in design and the variables utilized as inputs for the proposed units are presented in Table 1.

Fig. 6(a) provides a comprehensive depiction of the average monthly electricity demand, denoted in kWh. The bar chart illustrates the amount of electricity consumed in each month, commencing at 636 kWh in January and progressively declining to 517 kWh in December. The average electrical demand, calculated to be over year, winter, spring, summer, and autumn are 452 kWh, 582 kWh, 443 kWh, 342 kWh, and 441 kWh, respectively, offering a consolidated representation of the overall energy usage pattern. While Fig. 6(b) shows the average monthly electrical demand in each season. These figures collectively provide valuable insights into the energy requirements and consumption patterns for pragmatic household applications throughout the year.

Table 2 presents the datasheet for the panels, offering a range of specifications. The nominal power of the BIPV/T equipment is indicated as 320 W, representing their maximum power output capacity. The module efficiency is stated as 16.94%, denoting the efficiency at which the panels convert sunlight into electrical energy. The panel area is specified as 1.95 m^2, indicating the physical dimensions of each panel. The rated voltage is noted as 36.5 V, while the rated current is mentioned as 8.78 A, providing information on the electrical characteristics of the solar module component under normal operating conditions. The open circuit voltage is designated as 45.2 V, illustrating the terminal voltage of the BIPV/T layout when the load connected is absent. The provided short-circuit current measures 9.25 A, signifying the peak current that could flow under short-circuit conditions. The positive temperature coefficient value is given as −0.37%/ °C, indicating the

Table 1
The input parameters to the BIPV/T system.

Operating Conditions			
Data	**Symbol**	**Unit**	**Value**
Ambient temperature	T_a	^oC	12–34
Ambient temperature at NOCT	$T_{a,NOCT}$	^oC	20
Solar radiation at NOCT	G_{NOCT}	W/m^2	800
Solar radiation	G	W/m^2	500–986
Solar radiation at STC conditions	G_{ref}	W/m^2	1000
Average wind speed	$\vec{V}$	m/s	4.72
Design Specification			
Nominal operating cell temperature	$T_{C,NOCT}$	^oC	46
Transmittance-absorptance product	$\tau\alpha$	-	0.9
Packing factor of PV cell	p_c	-	0.95
Thickness of the material	Δx	m	0.04
Thermal conductivity of panel	K_c	$W/m.^oC$	885
Area of the panel	A_p	m^2	1.95
PV module efficiency	η_m	-	0.1649
Inlet temperature	T_i	^oC	29
Outlet temperature	T_o	^oC	38.26
Mass flow rate	$\dot{m}$	Kg/s	0.05
Specific Heat	c_p	J/g^oC	4.18
PV rated power	P_m	W	320
Reference temperature	T_{ref}	^oC	25
Temperature coefficient	K_T	$1/^oC$	-3.7×10^{-3}
Average electrical demand	E_{ele}	kWh	452
Annual working hours	τk	hour	3600
Operating hours	OH	h	24
Daily hot water demand	HW_d	m^3/d	0.33
Number of storage hours	SH	h	8

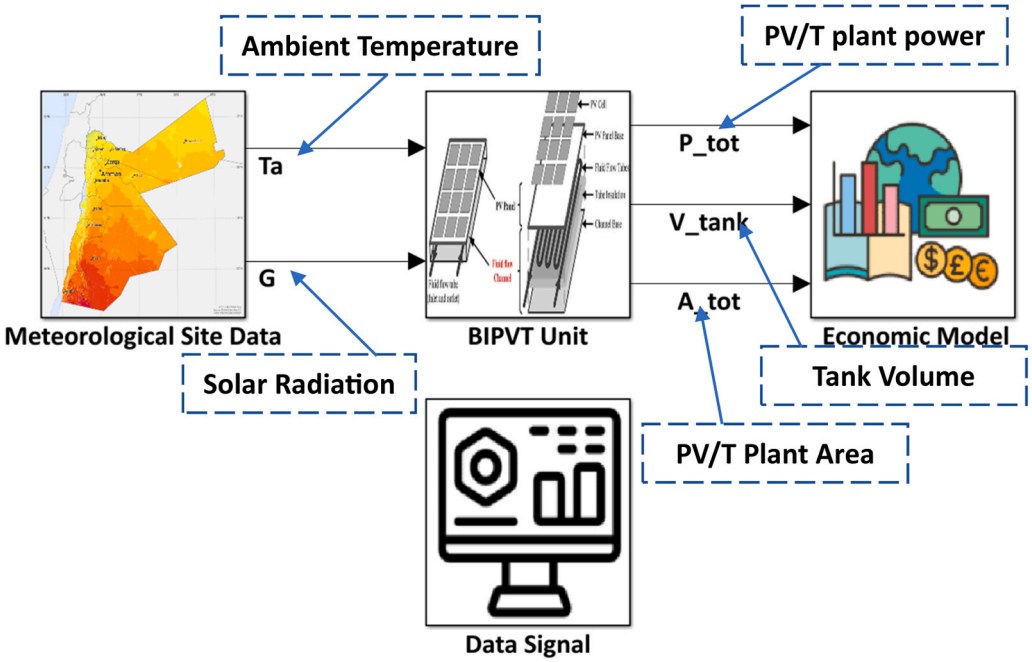

Fig. 5. The developed model browser in the MATLAB/Simulink® toolbox environment.

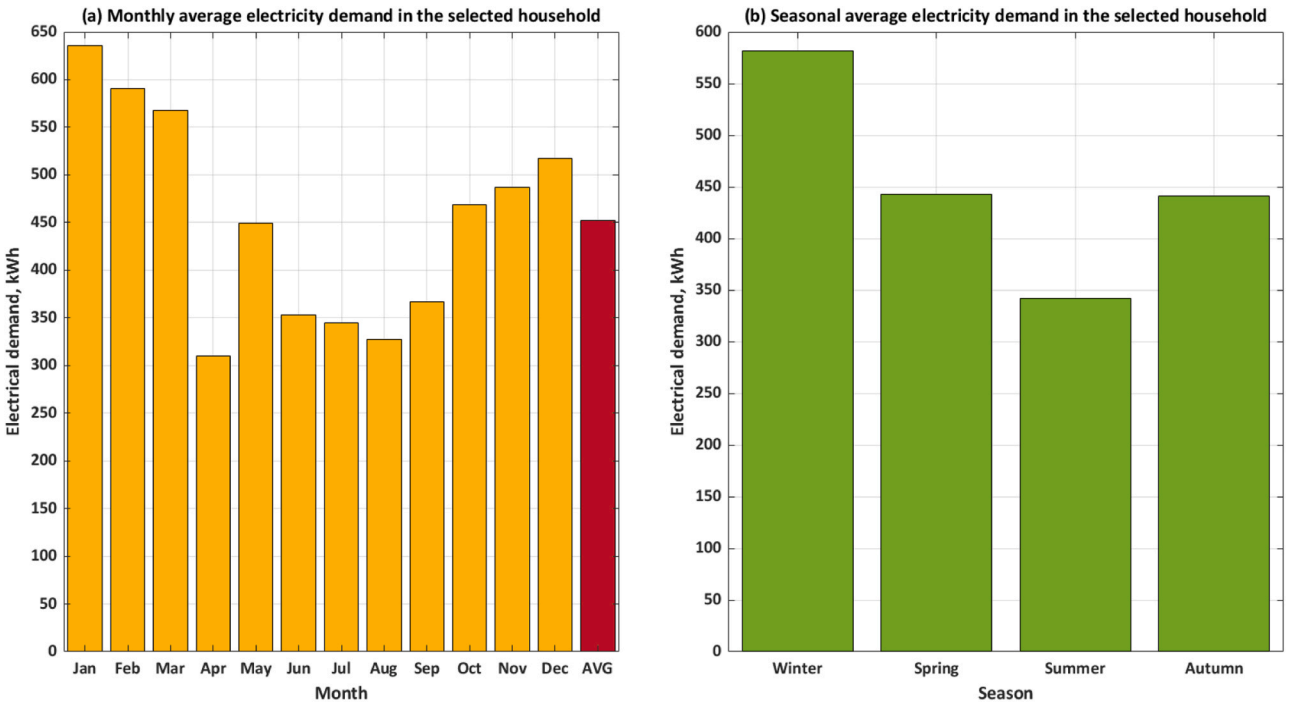

Fig. 6. Average electricity demand in the selected household: (a) Annual and (b) Seasonal.

Table 2
The BIPV/T panel datasheet [36].

Parameter	Symbol	Unit	Value
PV rated power	P_m	W	320
PV module efficiency	η_m	%	16.49
Current, maximum power point	I_{mp}	A	8.78
Voltage, maximum power point	V_{mp}	V	36.5
Current, short circuit	I_{sc}	A	9.25
Voltage, open circuit	V_{oc}	V	45.2
Number of cells	N_{cell}	-	72
Temp. Coefficient of Power	K_p	$\%/K$	-0.45
Temp. Coefficient of I_{sc}	K_I	$\%/K$	0.05
Temperature coefficient	K_T	$\%/^oC$	-0.37
Width	W	m	0.992
Thickness of the material	Δx	m	0.04
Length	L	m	1.96

drop in panel efficiency for each degree of temperature elevation. These parameters provide a detailed comprehension of the BIPV/T apparatus power output, efficiency, physical dimensions, electrical properties, and performance under varying temperature conditions.

2.4. Mathematical modeling

This section introduces a proposed mathematical model in MATLAB/Simulink® that expresses the implication of solar irradiation and ambient temperature on the performance of a BIPV/T system. The numerical simulation assessment reveals that the solar radiation is the most influenced parameter, followed by temperature. The quantitative analysis is derived from a typical BIPV/T system with a 320 W rated capacity in Mafraq, Jordan. The developed model used for calculations can be run to analyze the techno-economic performance of the BIPV/T systems and provides a foundation for the findings and conclusions of the current research. The PV cells' temperature before the cooling, ^oC, is given as follows [49]:

$$T_C = T_a + \frac{G}{G_{NOCT}}\left(T_{C,NOCT} - T_{a,NOCT}\right)\left(1 - \frac{\eta_m}{\tau\alpha}\right) \quad (1)$$

where, $T_{a,NOCT}$ is the ambient temperature equals to 20°C, G_{NOCT} denotes the solar radiation defined as 800 W/m^2 at NOCT conditions, and $\tau\alpha$ stands for the effective transmittance-absorptance product and is set at 0.90 [50].

The heat transfer loss from the BIPV/T module, is evaluated based on the following formula [50]:

$$Q_m = \left(h_c + \left(\frac{K_c}{\Delta x}\right)\right) \times A_p \times (T_C - T_a) \quad (2)$$

As stated by Ref. [51], the heat transfer coefficient, h_c, $W/m^2.^oC$, is introduced specifically relevant to a wind speed of $\vec{V} = 4.72$ m/s:

$$h_c = 5.67 + \left(3.86 \times \vec{V}\right) \quad (3)$$

Total solar energy absorbed by the BIPV/T module, is found as follows [52]:

$$E_m = p_c \times \tau\alpha \times G \times A_p \quad (4)$$

The calculation of the absorbed thermal energy, by the water, involves [52]:

$$E_{th} = \dot{m} \times c_p \times (T_o - T_i) \quad (5)$$

Thermal efficiency is evaluated using the following expression [52]:

$$\eta_{th} = \frac{E_{th}}{E_m} \quad (6)$$

Thermal power output from BIPV/T unit, is calculated from Eq. (7) as given:

$$P_{th} = E_m \times \eta_{th} \quad (7)$$

Electrical PV module output power, is calculated using the equation below [53]:

$$P_{PV} = P_m \times \frac{G}{G_{ref}} \times \left[1 + K_T \times \left(T_a + \left[G \times \frac{T_{C,NOCT} - 20}{800}\right] - T_{ref}\right)\right] \quad (8)$$

where, K_T is the temperature coefficient, 1/ °C, which equals -3.7×10^{-3}, G_{ref} is the solar radiation at STC conditions of 1000 W/m^2 and G is

the predicted solar radiation in W/m^2.

The cells' temperature after cooling, °C is obtained by Eq. (9) as proposed [54]:

$$T_{cool} = T_C - \frac{P_{th}}{1000 \times \dot{m} \times c_p} \tag{9}$$

The electrical efficiency is estimated in the following equation [55]:

$$\eta_{ele} = \frac{P_{ele}}{P_{PV}} \tag{10}$$

Thus,

$$P_{ele} = \frac{E_{ele}}{OH} \tag{11}$$

The overall BIPV/T layout efficiency is given based on the following expression [55]:

$$\eta_{PVT} = \frac{P_{th} + P_{ele}}{P_{PV}} \tag{12}$$

The number of PV/T modules that would be needed to cover the electrical demand can be estimated using the following correlation:

$$N_{PVT} = \frac{P_{PV}}{P_{ele}} \tag{13}$$

Thence, the total BIPV/T plant electrical power, is evaluated as follows:

$$P_{PV,tot} = N_{PVT} \times P_{PV} \tag{14}$$

The net BIPV/T plant thermal power, of the assembled plant, is expressed as:

$$P_{th,tot} = P_{th} \times N_{PVT} \tag{15}$$

The total BIPV/T plant area, is given as:

$$A_{tot} = A_p \times N_{PVT} \tag{16}$$

The PV/T plant efficiency can be calculated based on the following [55]:

$$\eta_{tot} = \frac{P_{th,tot} + P_{ele}}{P_{PV,tot}} \tag{17}$$

The actual overall output power, of the BIPV/T plant arrays, is demonstrated as [55]:

$$P_{tot} = P_{PV,tot} \times \eta_{tot} \tag{18}$$

Total energy generation per year, can be given as:

$$E_{tot} = \frac{P_{tot} \times \tau k}{1000} \tag{19}$$

The net storage tank volume capacity, can be computed by the relation below:

$$V_{tank} = \frac{HW_d \times SH}{A_{tot} \times \eta_{th}} \tag{20}$$

2.5. Economic analysis model

The cost-effectiveness of the BIPV/T system is examined based on the total Levelized Cost of Energy ($LCOE_{tot}$), *$/kWh*. These economic indicators are evaluated from Eq. (21) to Eq. (29). Accordingly, the following assumptions have been made: BIPV/T lifetime is 20 years, the interest rate is 5%, variable operating cost for the system is 0.1 $/kWh. Table 3 presents the parameters and indices related to the economic model. This analysis shows that the BIPV/T system is a cost-effective way to generate electricity for the required residential building. The sugeested BIPV/T system is expected to save the homeowner money on electricity bills and has a desirable $LCOE_{tot}$.

Table 3
The considered economic model parameters [56].

Input economic parameters		
Parameter	**Value**	**Symbol**
Number of operating years, *year*	20	n
Annual interest rate, %	5	i_r
Variable operating cost, *$/kWh*	0.1	VOC_{tot}
Load factor for system	0.9	f
Direct costs		
Storage tank cost, *$*	See Eq.(21)	X_{tank}
Inverter/controller cost, *$/kW*	180	X_{inv}
PV/T panel cost, *$/m^2*	200	X_{PVT}
Indirect costs		
Fixed O&M cost coefficient	0.02	y_k

The capital cost of the storage tank component, could be anticipated as a function of its storage volume based on the correlation below [56]:

$$X_{tank} = 494.9 + 808 \times V_{tank} \tag{21}$$

Total direct capital costs of the BIPV/T system's parts, can be obtained as [57]:

$$X_{c,tot} = X_{tank} + X_{PVT} \times A_{tot} + X_{inv} \times \left(\frac{P_{tot}}{1000}\right) \tag{22}$$

The annualized capital costs are calculated based on the amortization factor, as follows [58]:

$$crf = \frac{i_r(1+i_r)^n}{(1+i_r)^n - 1} \tag{23}$$

Annualized capital cost is determined as given [59]:

$$X_{Ann}^{CL} = crf \times X_{c,tot} \tag{24}$$

Total operation and maintenance costs of the BIPV/T system is expressed as [56]:

$$X^{OM} = (y_k) \times X_{c,tot} \tag{25}$$

Annualized operation and maintenance costs is computed as [45]:

$$X_{ann}^{OM} = X^{OM} \times crf \tag{26}$$

The total initial cost, *$/year*, can be calculated as [45]:

$$(X_{tot}) = \left(X_{Ann}^{CL}\right) + \left(X_{ann}^{OM}\right) \tag{27}$$

The total hourly cost of the plant is calculated as [58]:

$$X_{hour} = \frac{X_{tot}}{\tau k} \tag{29}$$

The total LCOE of the thermal-electrical power plan can be calculated as [45]:

$$LCOE_{tot} = \frac{(X_{hour})}{f \times P_{tot}} + VOC_{tot} \tag{29}$$

2.6. Multi-objective optimization using genetic algorithm

The genetic algorithm is an optimization tool that draws inspiration from nature and attempts to deliver high-quality solutions for troublesome issues within an adequate timeframe [60]. In general, it involves a metaheuristic concept and works with a set of humans, where each person is symbolized by a mathematical relation. For the initial period, an arbitrary individual is created, and then their fitness is monitored. These individuals are modified using both mutation and crossover operations, thus yielding emergence to offspring [60]. The fitness of all offspring is also checked, and the most prospective individuals are designated to build the following generation. This iterative procedure persists until either the highest number of generations is reached, coupled with data modifications, or the convergence requirements are

met, indicating that the optimization problem has been solved.

The genetic algorithm is well-suited for dealing with multi-objective optimization operations. It can handle conflicting objectives by employing the non-dominated sorting genetic algorithm-II (NSGA-II) and assessing individuals based on multiple fitness functions, resulting in a set of Pareto optimal solutions [61]. By fostering diversity and convergence, the algorithm effectively explores trade-offs and provides decision-makers with a variety of optimal solutions to select from. This makes the genetic algorithm an invaluable tool for real-world problems that encompass multiple objectives [62]. In this investigation, the optimization problem involves maximizing η_{tot} and P_{tot} while minimizing A_{tot}, and the genetic algorithm solver is used to identify the best solution. The Technique for Order of Preference by Similarity to Ideal Solution (TOPSIS) method, frequently applied which is utilized to adopt the obtained optimal solutions.

3. Results and discussion

To achieve the desired design outcomes, it is essential to assign the most suitable operating conditions. This system model encompasses all the design aspects calculated in this study to determine the total plant productivity. For example, a high productivity rate may lead to a larger plant area and higher costs. Consequently, the system units with the most significant impact are optimized to ensure the best operating conditions.

3.1. Performance analysis of the proposed BIPV/T system

Fig. 7(a) provides a comprehensive visual representation of the thermal efficiency, electrical efficiency, and overall efficiency of the system across different seasons. The data showcases the system's impressive performance, adaptability, and capacity to maximize energy

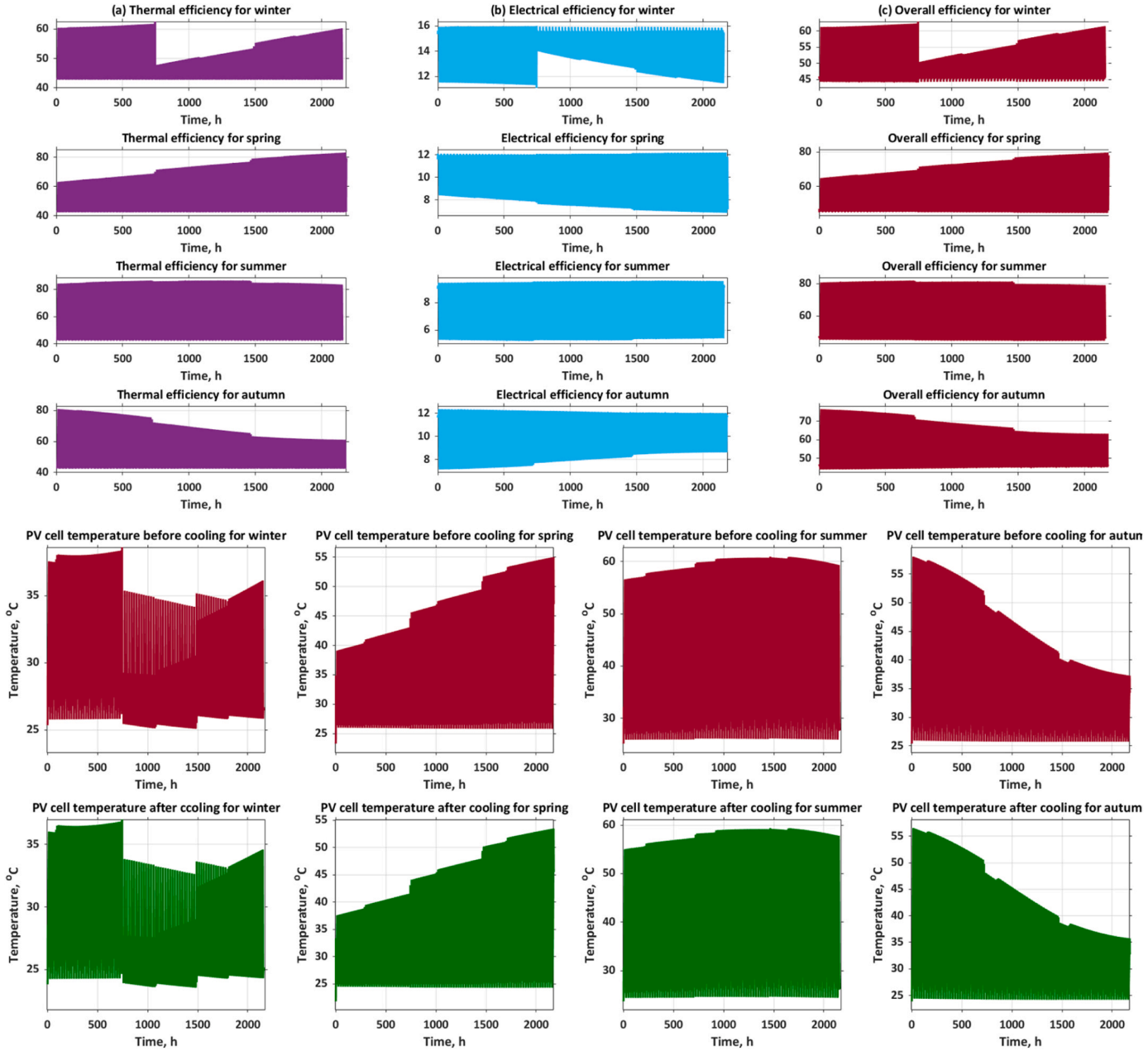

Fig. 7. (a) Thermal efficiency, (b) Electrical efficiency, and (c) Overall efficiency of the system in different seasons. (d). PV cell temperature before versus after cooling through different seasons.

conversion, with notable variations depending on the environmental conditions of each season. In accordance the thermal analysis model based on Eq. (6), the proposed BIPV/T system exhibits a notable optimal and stable thermal efficiency during the summer season. Hence, it can be seen that the maximum thermal efficiency of the BIPV/T system in the summer at middle of the season obtained by the applied dynamic approach is about 86.4%, considering input parameters of the BIPV/T system that presented in Table 1. In contrast, the winter season shows the maximum thermal efficiency at 62.2%, with a minimum of 48.4% at the beginning of February. To that end, during summer, the system maintains exceptional thermal efficiency, consistently exceeding 80%. Such a high performance level emphasizes the notable system's capability to utilize thermal energy during the warmer season. Also, this shows the capacity of the system to optimize its energy conversion through summer months. Interestingly, the spring and autumn seasons exhibit moderate thermal efficiency, In spring, the thermal efficiency varies between 60% and 80%, presenting the system's flexibility to changing environmental conditions. During summer, the system maintains exceptional thermal efficiency, consistently exceeding 80%. Such a high performance level emphasizes the notable system's capability to utilize thermal energy during the warmer season. Whereas, in autumn, the system's thermal efficiency remains consistently strong, ranging between 60% and 80%.

Fig. 7(b) illustrates the seasonal variation of electrical efficiency, calculated according to Eq. No. (10). It is revealed that the proposed BIPV/T system within winter season boasts a robust electrical performance with stable peak values throughout the season. During winter, the system exhibits an electrical efficiency of approximately 15.98% and then decreases to around 13.96% at 768 hours due to reduced thermal efficiency, emphasizing its ability to convert thermal energy into usable electrical power. While in summer season, the electrical efficiency lowers further to approximately 9.6o% and then decreases to around 5.3% at 1500 hours, reflecting the challenges posed by higher temperatures on energy conversion. However, even with this reduction, the system remains capable of delivering a noteworthy electrical output. In addition, the electrical efficiency of the system in spring season slightly decreases to around 12.2%, indicating a slight reduction in the conversion process. With a gradual decrease in ambient temperatures in autumn, the electrical efficiency shows a modest increase back to approximately 12.4% and decreases to 7.5% due to similar reasons as spring, but with less pronounced effects, signifying the system's ability to adapt and optimize performance in changing conditions.

To assess the overall efficiency of the system, we consider the combined performance of thermal and electrical efficiency, as illustrated in Fig. 7(c). Therefore, Fig. 7(c) is the comparison of overall efficiency in Mafraq in four seasons: winter, spring, summer, and autumn. As can be seen in Fig. 7(c), the overall efficiency of the BIPV/T system is highest in spring and summer, at around 80%. It is the lowest in winter, at around 63%. As summer arrives, the overall efficiency stabilizes at a commendable 82%, highlighting the system's exceptional ability to convert energy efficiently during the hottest season. This suggests a harmonious synergy between the thermal and electrical components of the system during colder months. Spring witnesses a varying overall efficiency ranging between 64.9% and 79.7%, showcasing the system's capacity to adapt to different temperature ranges. However, during autumn, the overall efficiency experiences a slight decrease, ranging between 76.3% and 62.9%, as the system adjusts to the changing climate conditions. From Fig. 7(c) it can be concluded that the overall efficiency are lower in winter and higher in summer. The explanation is that the solar altitude is elevated during summer as opposed to winter.

Fig. 7(d) presents a visual representation of the PV cell temperature both before and after the cooling process across different seasons. The data provides valuable insights into the temperature dynamics experienced by the PV cells throughout the year. During winter, the PV cell temperature, prior to cooling, reaches its lowest point at approximately 38.4℃. However, after the cooling process is implemented, the temperature is further reduced to nearly 36.8℃. This significant reduction in temperature demonstrates the effectiveness of the cooling system in maintaining optimal operating conditions for the PV cells during the colder season.

Conversely, the summer season presents an interesting contrast. The PV cell temperature before cooling reaches its peak, reaching around 60.9℃. The high temperature highlights the challenges posed by the intense summer heat to the efficient operation of the PV cells. However, with the implementation of the cooling system, the temperature experiences a decrease to approximately 59.3 ℃. Spring and autumn are highlighted as optimal periods for efficiency, which demonstrate a consistent 2°C decrease in cell temperature after cooling. This equally successful outcome emphasizes the moderate ambient temperatures and solar irradiance during these seasons, enabling the cooling system to function at its highest efficiency level. Ultimately, it can be concluded that before cooling, the PV cell temperature is highest in summer and lowest in winter, as expected. After cooling, the temperature difference between seasons is smaller, but summer temperatures are still the highest and winter temperatures are still the lowest. Fig. 7(d) thus emphasizes the importance of cooling mechanisms in regulating the temperature of PV cells in different seasons.

Fig. 8 presents a visual representation of the number of modules required and the total plant area needed across different seasons. The data offers valuable insights into the spatial requirements of the system throughout the year. During winter, the system demonstrates its efficiency by requiring a relatively smaller plant area of approximately 17.4 m^2. This compact footprint showcases the system's ability to optimize space utilization during the colder season. Correspondingly, the number of modules required is around 9, highlighting the system's ability to generate substantial energy output within a limited area.

Conversely, the summer season presents a contrasting scenario. With the heightened energy demands and more intense sunlight, the system necessitates a larger plant area to accommodate the increased energy production. In this case, the plant area required reaches its peak at approximately 37.5 m^2, reflecting the system's need for a larger installation space to harness the abundant solar resources during the hotter months. Consequently, the total number of PV/T modules (Fig. 8(a)) follows a dual pattern in winter, which peak with 9 PV/T units. In contrast, summer exhibits considerably higher deployment, with 19 unit. Moreover, the results for the proposed BIPVT system with spring and autumn seasons indicate the average maximum number of units, is estimated as 14 and 15 PV/T unit, respectively. This trend suggests a prioritization of PV/T utilization during seasons with moderate solar irradiance and ambient temperatures. This knowledge enables effective planning and allocation of resources to ensure optimal energy generation throughout the year.

The overall output power and the total plant efficiency are depicted in Fig. 9(a) and (b), respectively. It is highly noted from Fig. 9(a) that the highest overall output power was achieved during the summer with an average of 6143 W. During spring and autumn, the highest values were achieved at the switching times from spring to summer and also from summer to autumn at 4669 W and 4477 W, respectively. The lowest seasonal output power values were reported in winter due to the low atmospheric temperatures and the cloudy sky. The lowest annual values of 2278 W were obtained during the middle of winter. For total efficiency, Fig. 9(b) reveals that the winter season has the highest thermal efficiency of approximately 65% because cooler temperatures minimize the thermal losses of the system. As spring and summer temperatures increase, there is a slight decrease in efficiency to lower than 60% because of the heightened dissipation of heat.

3.2. Cost analysis findings

In general, a cost evaluation is carried out to provide an estimation of the system's economic competitiveness. The cost results of Mafraq in the four annual seasons are presented in Fig. 10. The economic findings

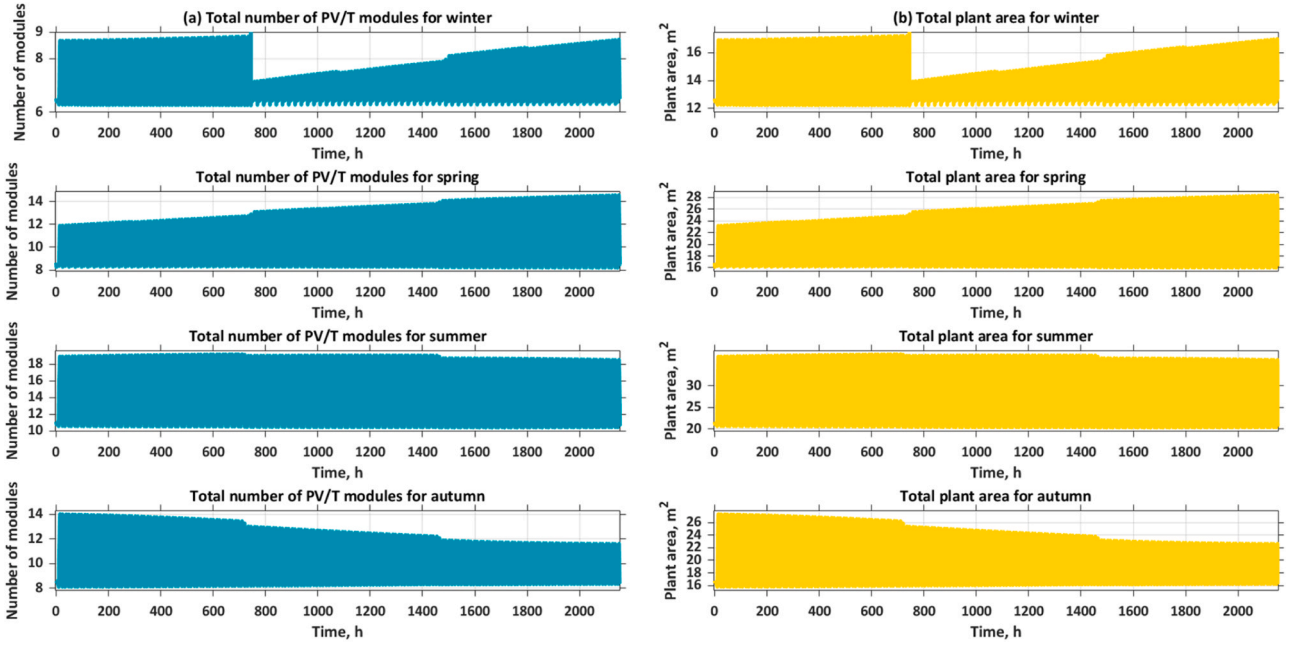

Fig. 8. (a) Total number of PV/T modules and (b) Overall plant area of the BIPV/T system during different seasons.

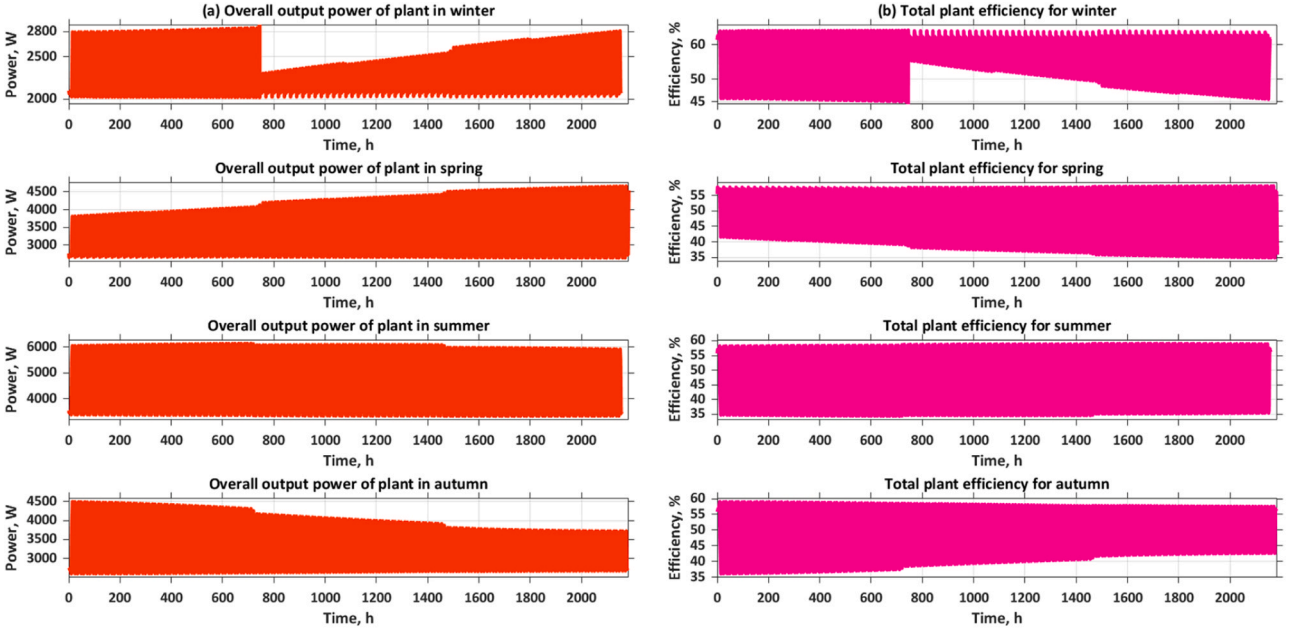

Fig. 9. The time-change of the BIPV/T system in the four annual seasons; (a) Overall output power; (b) Total efficiency.

unveiled that the LCOE of the suggested BIPV/T system is estimated about 0.10 $/kWh consistently across all the year seasons, The considering economic model parameters that demonstrated in Table 3. Therefore, it indicates that the system is highly competitive with other renewables and has great potential for implementation in the adopted location throughout the year.

3.3. Sensitivity analysis results

Fig. 11 displays the total module number and total surface area profiles of the BIPV/T plant with respect to solar radiation and ambient temperature. It is seen in Fig. 11 that the solar flux uniformity and level rates of solar flux increase with increasing both the total module number and total surface area of the BIPV/T plant. This is attributed to the higher rates of solar irradiation falling on the PV modules by increasing the total modules number and total surface area, which increases the total thermal heat gain acquired by the plant and thus increases the electrical and thermal performances of the plant. It is concluded that the optimum total modules number and total surface area of the BIPV/T plant should be desired as 16 modules and 30 m^2, corresponding to total solar irradiation and ambient of 1000 W/m^2 and 34 °C, respectively.

temperature.

The generated electric power produced by the BIPV/T plant is influenced by two pivotal parameters; namely, solar irradiation and environmental temperature. Fig. 12 illustrates the output power and total efficiency for the BIPV/T plant at different values of solar

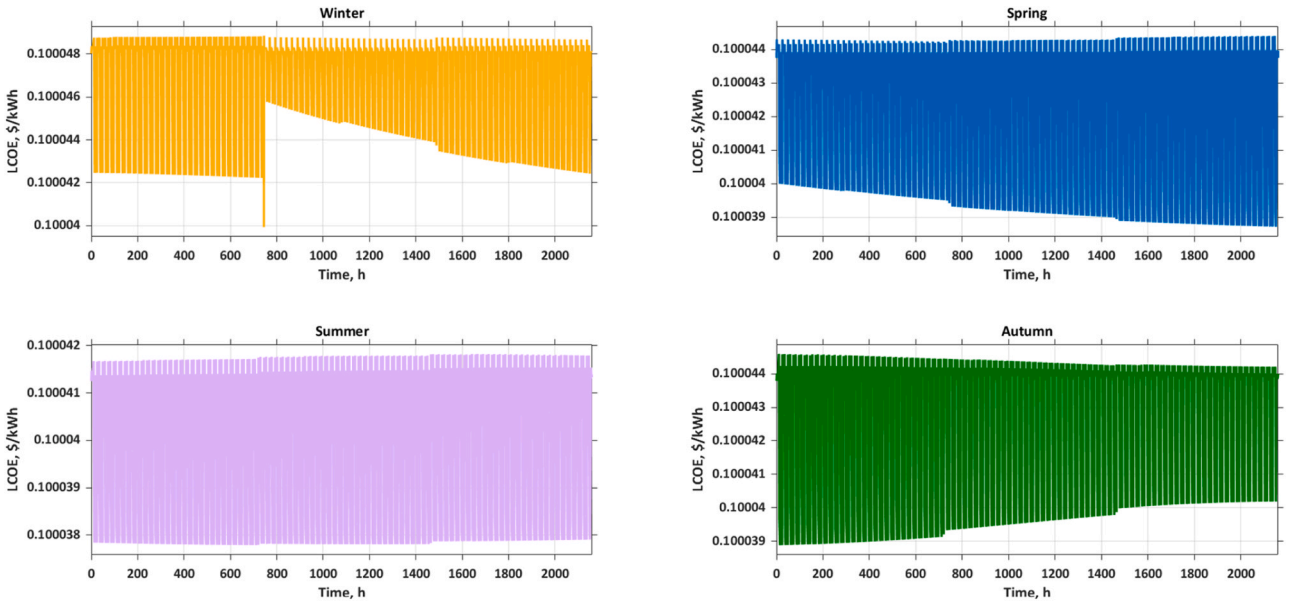

Fig. 10. Time-changes of the levelized cost of energy for the proposed system in the four annual seasons.

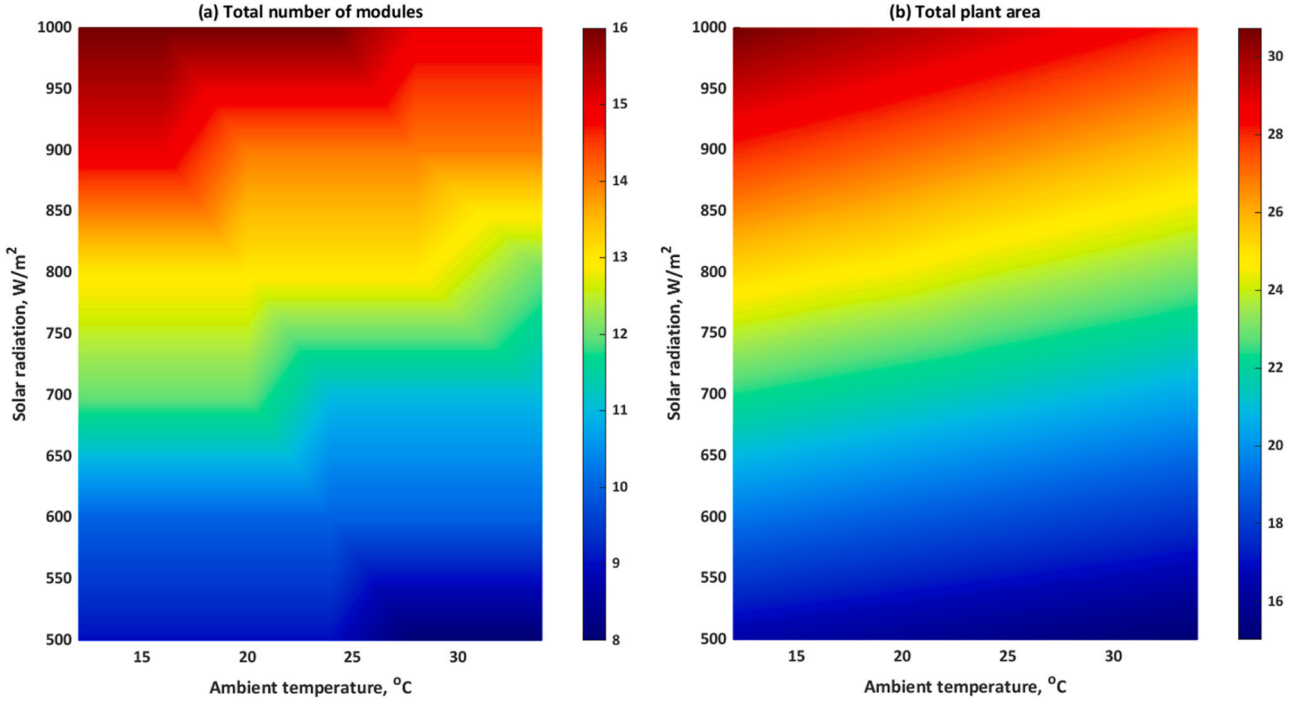

Fig. 11. Sensitivity analysis finding: (a) Total modules number profile of the BIPV/T plant with respect to solar radiation and ambient temperature; (b) Total plant area profile concerning solar radiation and ambient.

irradiance and climate temperature, respectively. Generally, it mainly shows that as the solar irradiance and climate temperature increase, the output power increases while the total efficiency for the BIPV/T plant decreases. The findings declared that higher levels of solar flux lead to higher electric output power of the BIPV/T plant due to the significant increase in thermal energy acquired by the BIPV/T. In contrast, it is seen that despite the electrical capacities augmentation of the BIPV/T plant with larger solar irradiation, the system's total efficiency decreases due to the significant increase in thermal energy acquired by the BIPV/T is lower compared to the increase in the system thermal losses dissipated by the BIPV/T plant, which may impede their potential for power generation among other solar power systems. The results show that the power attained by the BIPV/T plant with solar flux values between 500 and 1000 W/m^2 is between 2.70 and 4.50 kW, corresponding to the system's overall efficiency between 60% and 36%, respectively. On the other hand, it is seen the effect of ambient temperature on the output power and total efficiency for the BIPV/T plant has the same trend as the influence of solar irradiation. This is attributed to the impact of those weather factors cannot be separately represented because the ambient temperature value is affected by the solar intensity in such selected sites. Upon the gained findings in Fig. 12 (a), Eq. (30) and Eq. (31) are formulated to compute the produced electric power and system efficiency of the suggested BIPV/T plant configuration as a function of the solar intensity, respectively.

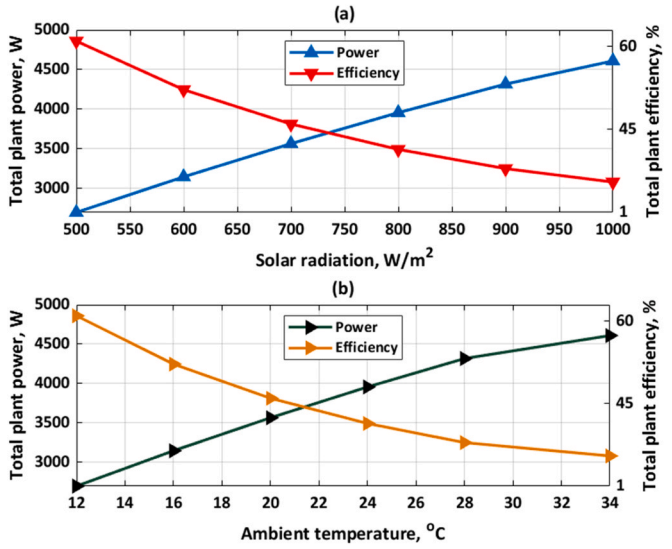

Fig. 12. Changes in overall plant efficiency and power output capacity versus solar radiation and ambient temperature.

$$P_{,total} = \left[5.80 * 10^{2} + 3.50 I_s + 2.40 * 10^{-3} {I_s}^{2} + 1.90 * 10^{-6} {I_s}^{3}\right] \quad (30)$$

$$\eta_{,total} = \left[5.20 - 0.01 I_s + 8.90 * 10^{-6} {I_s}^{2} - 2.80 * 10^{-9} {I_s}^{3}\right] \quad (31)$$

Similarly, the obtained results in Fig. 12 (b), the produced electric power and system efficiency of the suggested BIPV/T plant configuration are formulated as a function of the ambient temperature, respectively, as presented in Eq. (32) and Eq. (33);

$$P_{,total} = \left[1.70 * 10^{3} + 44.0 T_a + 4.10 {T_a}^{2} + 0.086 {T_a}^{3}\right] \quad (32)$$

$$\eta_{,total} = \left[3.40 - 0.15 T_a + 0.0035 \quad {T_a}^{2} - 2.60 * 10^{-5} \quad {T_a}^{3}\right] \quad (33)$$

Table 4 provides the impact of variations in equipment costs on LCOE within the framework of this research. The table contains baseline costs for the key components of the proposed model, such as the storage tank, inverter/controller, and PV/T panel. In this regard, the corresponding LCOE values are calculated at different percentage variations including +20%, −20%, +40%, and −40%. The fluctuations denote potential alternations in costs, which allow a robust exploration of the sensitivity of LCOE to changes in equipment expenses. This detailed breakdown aims to contribute valuable insights into the economic dynamics of the developed system.

3.4. Multi-objective optimization analysis by genetic algorithm

In the optimization problem, a multi-objective optimization using the NSGA-II method is also conducted for the minimization of the total BIPV/T plant area and maximization of the total efficiency and net thermal power of the system as well as to estimate the optimized operating conditions for input variables across different seasons within the provided ranges that provided in Table 1, Table 2, and Table 3. The optimized operating conditions for the input variables are to be estimated for different seasons. Thus, the multi-objective optimization is formulated including the operating ranges of the input variables, and is solved by the NSGA-II method of genetic algorithm using the default ranges for the parameters as provided in MATLAB. The optimal solutions are obtained corresponding to the winter, spring, summer, and autumn seasons and the optimal solution is selected by the TOPSIS decision maker.

Fig. 13 (a-d) presents the optimal solutions achieved after solving the multi-objective optimization problem for the winter, spring, summer, and autumn seasons respectively. The red spheres indicate the optimal solutions achieved after solving the multi-objective optimization problem whereas the green sphere is the optimal solution selected by the TOPSIS technique. Referring to

Figure (a), the optimal solution for the winter season for the BIPV/T system indicates that A_{tot} = 32.89 m^2, η_{tot} = 63% and P_{tot} = 5320 W, respectivelly, can be achieved corresponding to the input variables as follows: N_{PVT} = 15 moduler, EC_{ele} = 21.95 kWh, $P_{PV,tot}$ = 2606 and $P_{th,tot}$ = 5569 W, respectivelly. Whereas, for spring season, the input variables (N_{PVT}, EC_{ele}, $P_{PV,tot}$, and $P_{th,tot}$) can be maintained at 12 module, 23.53 kWh, 1371 W, and 3367 W, respectively to obtain optimal values for A_{tot}= 20.85, η_{tot} = 64.2% and P_{tot} = 3234 W, respectivelly. Similarly, for summer season, the optimal solution (A_{tot} = 28.59 m^2, η_{tot} = 64.2% and P_{tot} = 4408 W) is obtained for N_{PVT} = 16 module, EC_{ele} = 23.63 kWh, $P_{PV,tot}$ = 1780 W and $P_{th,tot}$= 4700 W, respectivelly. Whereas, for autumn season, the input variables (N_{PVT}, EC_{ele}, $P_{PV,tot}$, and $P_{th,tot}$) can be maintained at 14 module, 21.84 kWh, 1416 W and 3368 W, respectively to obtain optimal values for A_{tot} = 20.91 m^2, η_{tot} = 63.3% and $P_{PV,tot}$ = 3252 W, respectivelly.

Ultimately, the obtained results in the multi-objective optimization problem for different seasons result from the system's physical characteristics and interactions. During winter, efficient operation is attained with more PV/T panels (N_{PVT}) and reduced electric power consumption (EC_{ele}), PV power output ($P_{PV,tot}$), and thermal power output ($P_{th,tot}$). It is revealed that the system undergoing spring optimization involves a balanced mix of input variables, while summer optimally utilizes higher N_{PVT} and $P_{th,tot}$, while moderate P_{ele} and $P_{PV,tot}$ are obtained. In autumn, moderate N_{PVT} and $P_{PV,tot}$ with lower P_{ele} and $P_{th,tot}$ lead to the best performance. These solutions aim to maximize energy capture and efficiency while minimizing power consumption for each season, considering varying solar conditions and energy needs. To assist the optimal design of the new-designed BIPV/T system, fitted curve is done to formulate regression equations, which are derived using the Pareto optimal points curve to determine a comprehensive objective function interacted the three examined objectives (total BIPV/T plant area A_{tot}, total plant efficiency η_{tot}, and net thermal power of the system P_{tot}) for the BIPV/T plant under the four investigated annual seasons. The derived regression equations of the concluded tri-objective functions are clearly highlighted in Appendix A, as a supplementary material.

4. Comparative discussion with published similar studies

The simulation results of this work are consistent with previously published findings reported by other scholars in the literature. Table 5 illustrates a comparative investigation between the recent study and other experimental and simulation studies related to BIPV/T system.

Table 4
Impact of equipment cost changes on the LCOE.

Equipment	Baseline cost	LCOE at Baseline ($/kW$_p$)	LCOE at (+20%) variation	LCOE at (-20%) variation	LCOE at (+40%) variation	LCOE at (-40%) variation
Storage tank cost, $	1067	0.1	0.12	0.08	0.14	0.06
Inverter/controller cost, $/kW	180					
PV/T panel cost, $/m^2	200					

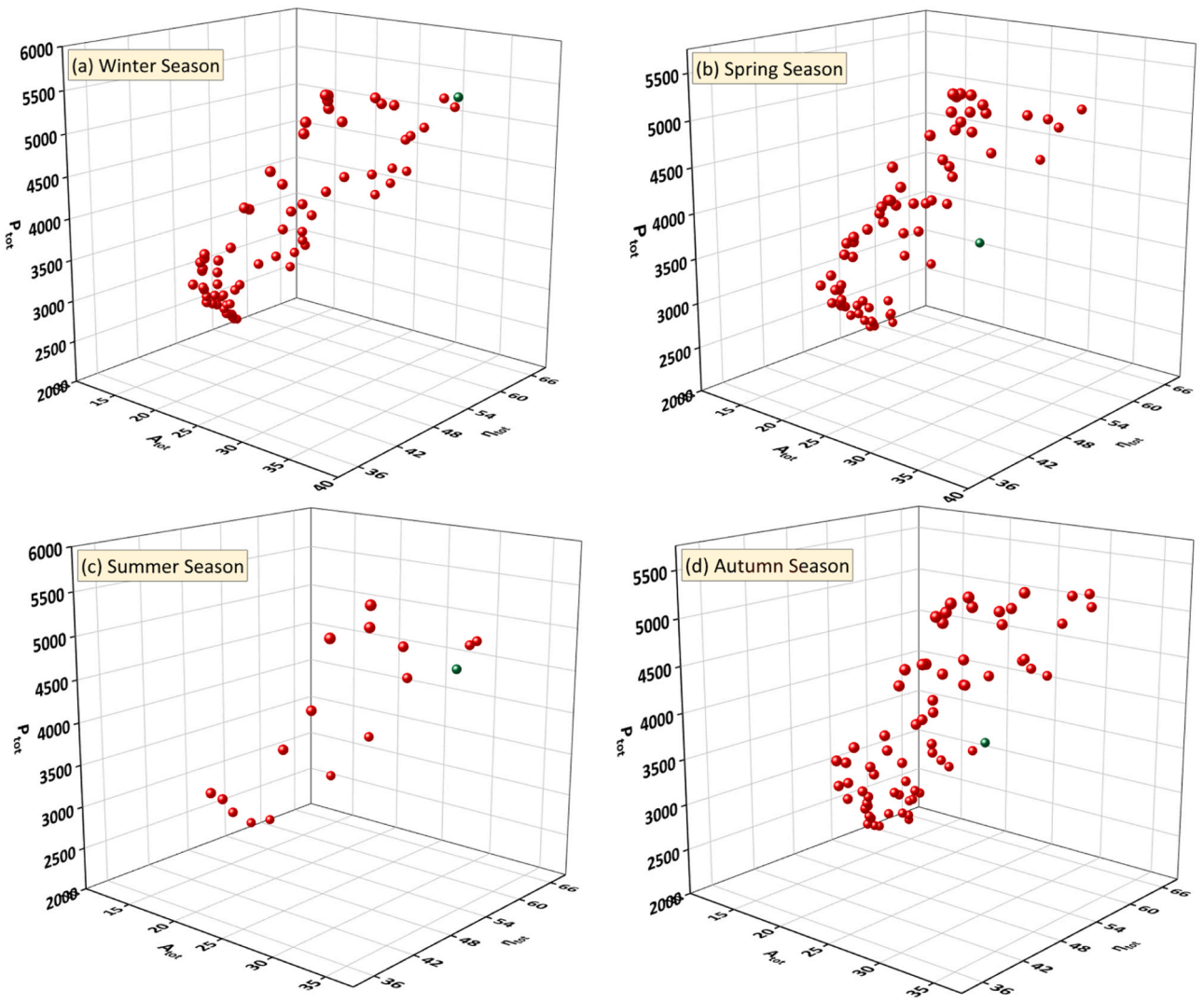

Fig. 13. Multi-objective optimization for minimizing A_{tot} and maximizing η_{tot} and P_{tot}over four seasons for the BIPV/T system, (a) Winter, (b) Spring, (c) Summer, and (d) Autumn. The optimal solution is shown by the green sphere.

Table 5
Comparative examination of the current work and other research on BIPV/T systems.

Performance Metric	Current study	Experimental study [63]	Simulation study [64]
System type	BIPV/T + storage tank	BIPV/T + heat pump	BIPV/T + solar thermal collector
System analysis	2-E	1-E	1-E
Simulation tool	MATLAB/ Simulink®	MATLAB	MATLAB
Climate conditions	Hot and arid	Mediterranean and mild	Humid and subtropical
Efficiency (thermal)	43.1%-62.2%	45.2%-64%	49.85%
Efficiency (electrical)	11.3%-15.98%	13.4%-14.2%	12.78%
Efficiency (overall)	44.2%-62.9% (winter) 79%-82% (summer)	70.7–83.7%	68.16%

5. Conclusions

This studuy introduces comprehensive theoretical dynamic modeling, seasonal performance optimization, and techno-economic analysis of a building integrated photovoltaic thermal (BIPV/T)) plant for providing both electricity and heating purposes in residential buildings. The investigation involved calculating various parameters, including panel temperature before and after cooling (e.g., before 65℃, after 58℃), electrical and thermal efficiencies (e.g., thermal efficiency in summer: >80%, overall efficiency in winter: 60%), thermal-electrical power production (e.g., power output with a solar flux of 1000 W/m^2: 4.50 kW), and the required plant size and area for a typical household (e.g., total modules number: 16 modules, total surface area: 30 m^2). Moreover, a multi-objective optimization based on a second non-dominated sorting genetic algorithm (NSGA-II) has been also implemented for simultaneously the total efficiency and net thermal power and minimizing of the total BIPV/T plant area. Pareto optimal frontier for each season is determined, considering the operational limits of input variables, solved using the NSGA-II genetic algorithm method, and the optimum solution is chosen by applying a TOPSIS decision-making approach. More so, the two-layer feed-forward back-propagation artificial neural network modeling is developed to accurately predict the hourly solar radiation and ambient temperature using historical meteorological data. The major results are summarized below:

1. The optimization findings indicated that the proposed NSGA-II shows a feasible method to attain maximum net thermal power

and optimal total efficiency of 5320 W and 63% with a minimal total plant area of 32.89 m^2 that attained a very low deviation index from the ideal solution if the BIPV/T plant is designed with $N_{PVT} = 15$ module, $EC_{ele} = 21.95$ kWh, $P_{PV,tot} = 2606$ and $P_{th,tot} = 5569$ W, respectively.

2. The cost-effectiveness of the BIPV/T system was examined through the Levelized Cost of Energy (LCOE) calculations, considering various economic indicators. The study found that the LCOE equals about 0.10 $/kWh and the system's overall efficiency varied with the changing seasons, with winter exhibiting the highest overall efficiency (e.g., 60%) and autumn experiencing a slight decrease in efficiency (e.g., 60–75%) due to changing climate conditions.
3. During the summer season, the importance of cooling mechanisms for regulating the PV cell temperature was emphasized, as high temperatures posed challenges to the efficient operation of the PV cells (e.g., PV cell temperature before cooling: 60℃, after cooling: 58℃). The study identified the optimum total modules number and total surface area for the BIPV/T plant under specific solar irradiation and ambient temperature conditions (e.g., 16 modules and 30 m^2 for 1000 W/m^2 solar irradiation and 34℃ ambient temperature).
4. Furthermore, the research revealed that higher solar flux levels led to increased electric output power of the BIPV/T plant due to a significant rise in thermal energy acquisition. However, the system's total efficiency decreased with larger solar irradiation, primarily due to increased thermal losses, which impacted its potential for power generation (e.g., power output with solar flux between 500 and 1000 W/m^2: 2.70–4.50 kW, overall efficiency: 36–60%).

In conclusion, the findings indicate that the suggested framework can be applicable to various building types and geographical locations. Consequently, it holds considerable value in advancing the utilization of solar energy with optimal energy, economic, and environmental performances.

6. Limitations and future recommendations

Overall, has the potential to usher in opportunities for contemporary polygeneration applications, contributing to improved living conditions in the MENA regions. However, it is crucial to consider certain challenges in the applicability of the proposed BIPV/T configuration as follows:

(1) It is imperative to conduct genuine experimental studies to authenticate and assess the actual potential as well as the long-term functionality of BIPV/T configurations in remote areas.
(2) In this context, the enhancement of BIPV/T systems' performance can be achieved through the adoption of innovative materials such as phase change materials (PCMs), solar concentrators, and extended heat transfer surfaces. Exploring the integration of various types of concentrative devices into buildings in a novel manner warrants further investigation.
(3) The effective implementation of BIPV/T systems requires consistent regulation and support from governmental bodies, decision-makers, and other stakeholders in technology, financial planning, and policy development. To incentivize appropriate measures for assessing building restoration costs, financial incentives and subsidies may be crucial.

Declaration of Competing Interest

The authors declared that there is no conflict of interest.

Acknowledgement

Authors would like to acknowledge the support of the Interdisciplinary Research Center for Sustainable Energy systems (IRC-SES), King Fahd University of Petroleum & Minerals (KFUPM), Dhahran, Saudi Arabia.

Appendix A

To assist the optimal design of the new-designed BIPV/T system, fitted curve is done to formulate regression equations, which are derived for the Pareto optimal points curve to determine a comprehensive objective function interacted the three examined objectives (total BIPV/T plant area A_{tot}, total plant efficiency η_{tot}, and net thermal power of the system P_{tot})under the different investigated seasons for the BIPVT plant.

Autumn season

Objective Function=-0.000056–1.000 A_tot + 1.000 eta_tot + 1.000 P_tot - 0.000003 A_tot*A_tot - 0.000013 eta_tot*eta_tot - 0.000000 P_tot*P_tot + 0.000001 A_tot*eta_tot + 0.000000 A_tot*P_tot - 0.000000 eta_tot*P_tot + 0.000000 A_tot*A_tot*A_tot + 0.000001 eta_tot*eta_tot*eta_tot + 0.000000 P_tot*P_tot*P_tot + 0.000001 A_tot*A_tot*eta_tot - 0.000000 A_tot*A_tot*P_tot + 0.000000 A_tot*eta_tot*eta_tot - 0.000000 A_tot*eta_tot*P_tot - 0.000000 eta_tot*eta_tot*P_tot + 0.000000 eta_tot*P_tot*P_tot (A1)

Winter Season

Objective Function=0.000002–1.000 A_tot + 1.000 eta_tot + 1.000 P_tot + 0.000000 A_tot*A_tot + 0.000000 eta_tot*eta_tot + 0.000000 P_tot*P_tot - 0.000000 A_tot*eta_tot −0.000000 A_tot*P_tot + 0.000000 eta_tot*P_tot - 0.000000 A_tot*A_tot*A_tot - 0.000000 eta_tot*eta_tot*eta_tot - 0.000000 P_tot*P_tot*P_tot - 0.000000 A_tot*A_tot*eta_tot + 0.000000 A_tot*A_tot*P_tot + 0.000000 A_tot*eta_tot*eta_tot + 0.000000 A_tot*eta_tot*P_tot - 0.000000 eta_tot*eta_tot*P_tot - 0.000000 eta_tot*P_tot*P_tot (A2)

Spring season

Objective Function=-0.000083–1.000 A_tot + 1.000 eta_tot + 1.000 P_tot - 0.000008 A_tot*A_tot + 0.000004 eta_tot*eta_tot - 0.000000 P_tot*P_tot + 0.000020 A_tot*eta_tot + 0.000000 A_tot*P_tot - 0.000000 eta_tot*P_tot + 0.000000 A_tot*A_tot*A_tot - 0.000003 eta_tot*eta_tot*eta_tot + 0.000000 P_tot*P_tot*P_tot + 0.000003 A_tot*A_tot*eta_tot - 0.000000 A_tot*A_tot*P_tot - 0.000002 A_tot*eta_tot*eta_tot - 0.000000 A_tot*eta_tot*P_tot + 0.000000 eta_tot*eta_tot*P_tot + 0.000000 eta_tot*P_tot*P_tot (A3)

Summer season

Objective Function=-0.000246–1.000 A_tot + 1.000 eta_tot + 1.000 P_tot + 0.000016 A_tot*A_tot - 0.000128 eta_tot*eta_tot + 0.000000 P_tot*P_tot + 0.000028 A_tot*eta_tot - 0.000000 A_tot*P_tot - 0.000000 eta_tot*P_tot - 0.000000 A_tot*A_tot*A_tot + 0.000023 eta_tot*eta_tot*eta_tot - 0.000000 P_tot*P_tot*P_tot + 0.000000 A_tot*A_tot*eta_tot + 0.000000 A_tot*A_tot*P_tot - 0.000008 A_tot*eta_tot*eta_tot + 0.000000 eta_tot*eta_tot*P_tot (A4)

References

[1] S.A.A. Mehrjardi, A. Khademi, S. Ushak, S. Alotaibi, Melting process of various phase change materials in presence of auxiliary fluid with sinusoidal wall temperatur, J. Energy Storage 52 (2022) 104779, https://doi.org/10.1016/j.est.2022.104779.

[2] R. Almodfer, M.E. Zayed, M.A. Elaziz, M.M. Aboelmaaref, M. Mudhsh, A. H. Elsheikh, Modeling of a solar-powered thermoelectric air-conditioning system using a random vector functional link network integrated with jellyfish search algorithm, Case Stud, Therm. Eng. 31 (2022) 101797.

[3] S.A. El-Agouz, M.E. Zayed, A.M. Abo Ghazala, A.R.A. Elbar, M. Shahin, M. Y. Zakaria, K.K. Ismaeil, Solar thermal feed preheating techniques integrated with membrane distillation for seawater desalination applications: Recent advances, retrofitting performance improvement strategies, and future perspectives, Process Safety Environ. Prot. 164 (2022) 595–612.

[4] A. Khademi, K. Shank, S.A.A. Mehrjardi, S. Tiari, G. Sorrentino, Z. Said, S. Ushak, A brief review on different hybrid methods of enhancement within latent heat storage systems, J. Energy Storage 54 (2022) 105362, https://doi.org/10.1016/j.est.2022.105362.

[5] M.M.M. Aboelmaaref, J. Zhao, W. Li, E.S. Ali, A.A.A. Askalany, M. Ghazy, L. Gu, M. E. Zayed, Research on solar dish/Stirling engine driven adsorption-based desalination system for simultaneous co-generation of electricity and freshwater: Numerical investigation, Case Stud. Therm. Eng. 47 (2023) 103044, https://doi.org/10.1016/j.csite.2023.103044.

[6] M.E.H. Attia, M.E. Zayed, A.E. Kabeel, A. Khelifa, M. Arıcı, M. Abdelgaied, Design and performance optimization of a novel zigzag channeled solar photovoltaic thermal system: Numerical investigation and parametric analysis, J. Cleaner Prod. 434 (2024) 140220.

[7] M. Abd Elaziz, et al., Machine learning-aided modeling for predicting freshwater production of a membrane desalination system: a long-short-term memory coupled with election-based optimizer, Alex. Eng. J vol. 86 (2024) 690–703.

[8] I.E. Agency, Global Energy Review: CO2 Emissions in 2021 Global emissions rebound sharply to highest ever level INTERNATIONAL ENERGY, 2021.

[9] M.I. El-Hadary, S. Senthilraja, M.E. Zayed, A hybrid system coupling zigzag type solar photovoltaic thermal collector and electrocatalytic hydrogen production cell: Experimental investigation and numerical modeling, Process Safety Environ. Prot. 170 (2023) 1101–1120.

[10] R. Dhivagar, S. Shoeibi, S.M. Parsa, S. Hoseinzadeh, H. Kargarsharifabad, M. Khiadani, Performance evaluation of solar still using energy storage biomaterial with porous surface: an experimental study and environmental analysis, Renewable Energy 206 (2023) 879–889.

[11] R. Mevada, H. Panchal, M. Ahmadein, M.E. Zayed, N.A. Alsaleh, J. Djuansjah, E. B. Moustafa, A.H. Elsheikh, K.K. Sadasivuni, Investigation and performance analysis of solar still with energy storage materials: An energy- exergy efficiency analysis, Case Stud. Therm. Eng. 29 (2022) 101687, https://doi.org/10.1016/j.csite.2021.101687.

[12] M.E. Zayed, M.M. Aboelmaaref, and, M. Chazy, Design of solar air conditioning system integrated with photovoltaic panels and thermoelectric coolers: Experimental analysis and machine learning modeling by random vector functional link coupled with white whale optimization, Therm. Sci. Eng. Prog. 44 (2023) 102051.

[13] A. Khelifa, A.E. Kabeel, M.E.H. Attia, M.E. Zayed, and M. Abdelgaied, Numerical analysis of the heat transfer and fluid flow of a novel water-based hybrid photovoltaic-thermal solar collector integrated with flax fibers as natural porous materials, Renewable Energy, vol. 217, p. 119245.

[14] M. Piratheepan, T.N. Anderson, Performance of a building integrated photovoltaic/thermal concentrator for facade applications, Sol. Energy vol. 153 (2017) 562–573, https://doi.org/10.1016/j.solener.2017.06.006.

[15] S. Shoeibi, H. Kargarsharifabad, S.A.A. Mirjalily, T. Muhammad, Solar district heating with solar desalination using energy storage material for domestic hot water and drinking water environmental and economic analysis, Sustain. Energy Technol. Assess. 49 (2022) 101713, https://doi.org/10.1016/j.seta.2021.101713.

[16] R.J. Yang, Overcoming technical barriers and risks in the application of building integrated photovoltaics (BIPV): Hardware and software strategies, Autom. Constr. vol. 51 (C) (2015) 92–102, https://doi.org/10.1016/j.autcon.2014.12.005.

[17] B. Hassan Al-Kbodi, T. Rajeh, M.E. Zayed, Y. Li, J. Zhao, J. Wu, Y. Liu, Transient heat transfer simulation, sensitivity analysis, and design optimization of shallow ground heat exchangers with hollow-finned structures for enhanced performance of ground-coupled heat pumps, Energy Build 305 (2024) 113870, https://doi.org/10.1016/j.enbuild.2023.113870.

[18] L. Mei, D.G. Infield, R. Gottschalg, D.L. Loveday, D. Davies, and, M. Berry, Equilibrium thermal characteristics of a building integrated photovoltaic tiled roof, Sol. Energy vol. 83 (10) (2009) 1893–1901, https://doi.org/10.1016/j.solener.2009.07.002.

[19] T. Yang, A.K. Athienitis, A review of research and developments of building-integrated photovoltaic/thermal (BIPV/T) systems, Renew. Sustain. Energy Rev. vol. 66 (2016) 886–912, https://doi.org/10.1016/j.rser.2016.07.011.

[20] B. Hassan Al-Kbodi, T. Rajeh, Y. Li, J. Zhao, T. Zhao, M.E. Zayed, Heat extraction analyses and energy consumption characteristics of novel designs of geothermal borehole heat exchangers with elliptic and oval double U-tube structures, Appl. Therm. Eng. 235 (2023) 121418, https://doi.org/10.1016/j.applthermaleng.2023.121418.

[21] M.E. Zayed, J. Zhao, A.H. Elsheikh, Y. Du, F.A. Hammad, L. Ma, A.E. Kabeel, S. Sadek, Performance augmentation of flat plate solar water collector using phase change materials and nanocomposite phase change materials: a review, Process Saf. Environ. Prot. 128 (2019) 135–157.

[22] A.M. Abdulateef, S. Mat, J. Abdulateef, K. Sopian, and, A.A. Al-Abidi, Geometric and design parameters of fins employed for enhancing thermal energy storage systems: a review, Renew. Sustain. Energy Rev. vol. 82 (no.) (2018) 1620–1635, https://doi.org/10.1016/j.rser.2017.07.009.

[23] T. Yang, A.K. Athienitis, A study of design options for a building integrated photovoltaic/thermal (BIPV/T) system with glazed air collector and multiple inlets, Sol. Energy vol. 104 (2014) 82–92, https://doi.org/10.1016/j.solener.2014.01.049.

[24] Y. Chen, K. Galal, and, A.K. Athienitis, Modeling, design and thermal performance of a BIPV/T system thermally coupled with a ventilated concrete slab in a low energy solar house: Part 2, ventilated concrete slab, Sol. Energy vol. 84 (11) (2010) 1908–1919, https://doi.org/10.1016/j.solener.2010.06.012.

[25] G.P. Hammond, H.A. Harajli, C.I. Jones, and, A.B. Winnett, Whole systems appraisal of a UK Building Integrated Photovoltaic (BIPV) system: Energy, environmental, and economic evaluations, Energy Policy vol. 40 (1) (2012) 219–230, https://doi.org/10.1016/j.enpol.2011.09.048.

[26] M. Koondhar, I. Laghari, B. Asfaw, R. Kumar, A.H. Lenin, Experimental and simulation-based comparative analysis of different parameters of PV module, Scientific African 16 (2022) 01197, https://doi.org/10.1016/j.sciaf.2022.e01197.

[27] S. Yang, F. Fiorito, D. Prasad, A. Sproul, and, A. Cannavale, A sensitivity analysis of design parameters of BIPV/T-DSF in relation to building energy and thermal comfort performances, J. Build. Eng. vol. 41 (2021), https://doi.org/10.1016/j.jobe.2021.102426.

[28] H. Chen, Z. Li, and, Y. Xu, Assessment and parametric analysis of solar trigeneration system integrating photovoltaic thermal collectors with thermal energy storage under time-of-use electricity pricing, Sol. Energy vol. 206 (no.) (2020) 875–899, https://doi.org/10.1016/j.solener.2020.06.046.

[29] S. Khanmohammadi, A. Shahsavar, Energy analysis and multi-objective optimization of a novel exhaust air heat recovery system consisting of an air-based building integrated photovoltaic/thermal system and a thermal wheel, Energy Convers. Manag. vol. 172 (2018) 595–610, https://doi.org/10.1016/j.enconman.2018.07.057.

[30] A. Shahsavar, P. Talebizadehsardari, and, M. Arıcı, Comparative energy, exergy, environmental, exergoeconomic, and enviroeconomic analysis of building integrated photovoltaic/thermal, earth-air heat exchanger, and hybrid systems, J. Clean. Prod. vol. 362 (June) (2022) 132510, https://doi.org/10.1016/j.jclepro.2022.132510.

[31] S.R. Asaee, S. Nikoofard, V.I. Ugursal, and, I. Beausoleil-Morrison, Techno-economic assessment of photovoltaic (PV) and building integrated photovoltaic/thermal (BIPV/T) system retrofits in the Canadian housing stock, Energy Build vol. 152 (2017) 667–679, https://doi.org/10.1016/j.enbuild.2017.06.071.

[32] A. Sohani, et al., The real-time dynamic multi-objective optimization of a building integrated photovoltaic thermal (BIPV/T) system enhanced by phase change materials, J. Energy Storage vol. 46 (2022), https://doi.org/10.1016/j.est.2021.103777.

[33] J. Bezaatpour, H. Ghiasirad, M. Bezaatpour, and, H. Ghaebi, Towards optimal design of photovoltaic/thermal facades: module-based assessment of thermo-electrical performance, exergy efficiency and wind loads, Appl. Energy vol. 325 (2022) 119785, https://doi.org/10.1016/j.apenergy.2022.119785.

[34] A. Buonomano, F. Calise, A. Palombo, and, M. Vicidomini, Transient analysis, exergy and thermo-economic modelling of façade integrated photovoltaic/thermal solar collectors, Renew. Energy (2019) 109–126, https://doi.org/10.1016/j.renene.2017.11.060.

[35] P. Gang, F. Huide, Z. Huijuan, and, J. Jie, Performance study and parametric analysis of a novel heat pipe PV/T system, Energy vol. 37 (1) (2012) 384–395, https://doi.org/10.1016/j.energy.2011.11.017.

[36] P. Gang, F. Huide, J. Jie, C. Tin-Tai, and, Z. Tao, Annual analysis of heat pipe PV/T systems for domestic hot water and electricity production, Energy Convers. Manag. vol. 56 (2012) 8–21, https://doi.org/10.1016/j.enconman.2011.11.011.

[37] A. Sohani, et al., Techno-economic evaluation of a hybrid photovoltaic system with hot/cold water storage for poly-generation in a residential building, Appl. Energy vol. 331 (2023), https://doi.org/10.1016/j.apenergy.2022.120391.

[38] Y. Abdalgadir, H. Qian, D. Zhao, A. Adam, and, W. Liang, Daily and annual performance analyses of the BIPV/T system in typical cities of Sudan, Energy Built Environ. vol. 4 (5) (2022) 516–529, https://doi.org/10.1016/j.enbenv.2022.04.001.
[39] C.F. Fu, Y. Ji, A. Alazzawi, M. Lu, B. Zhao, Q. Luo, Utilization of least squares support vector machine for predicting the yearly exergy yield of a hybrid renewable energy system composed of a building integrated photovoltaic thermal system and an earth air heat exchanger system, Eng. Anal. Bound. Elem. 152 (2023) 293–300.
[40] B. Zazoum, Solar photovoltaic power prediction using different machine learning methods, Energy Rep. 8 (2022) 19–25.
[41] A.E.H. Khandakar, M. Chowdhury, M. Khoda Kazi, K. Benhmed, F. Touati, M. Al-Hitmi, et al., Machine learning based photovoltaics (PV) power prediction using different environmental parameters of Qatar, Energies 12 (2019) 2782, https://doi.org/10.3390/en12142782.
[42] R. Rostamzadeh-Renani, M. Baghoolizadeh, S. Mohammad Sajadi, M. Pirmoradian, M. Rostamzadeh-Renani, S. Baghaei, S. Salahshour, Prediction of the thermal behavior of multi-walled carbon nanotubes-CuO-CeO2 (20-40-40)/Water hybrid nanofluid using different types of regressors and evolutionary algorithms for designing the best artificial neural network modeling, Alex. Eng. J. 84 (2023) 184–203, https://doi.org/10.1016/j.aej.2023.10.059.
[43] P.W. Tien, S. Wei, J. Darkwa, C. Wood, J.K. Calautit, Machine learning and deep learning methods for enhancing building energy efficiency and indoor environmental quality – a review, Energy and AI 10 (2022) 100198.
[44] B. Shboul, Techno-economic Modelling and Multi-Objective Optimisation of a New Stand- alone Hybrid CPSD-SE/HWT System in Microgrids Power Generation Under Jordan Climatic Conditions, The University of Sheffield (2021) [Online]. Available: https://etheses.whiterose.ac.uk/30596/.
[45] B. Shboul, et al., Design and Techno-economic assessment of a new hybrid system of a solar dish Stirling engine integrated with a horizontal axis wind turbine for microgrid power generation, Energy Convers. Manag. vol. 245 (2021), https://doi.org/10.1016/j.enconman.2021.114587.
[46] B. Shboul et al., Multi-Objective Optimal Performance of a Hybrid CPSD-SE/HWT System for Microgrid Power Generation, in Applications of Nature-Inspired Computing in Renewable Energy Systems, Mohamed Arezki Mellal, Ed. IGI Global Publisher of Timely Knowledge, 2021, pp. 166–210. doi: 10.4018/978-1-7998-8561-0.ch009.
[47] B. Shboul, et al., A new ANN model for hourly solar radiation and wind speed prediction: a case study over the north & south of the Arabian Peninsula, in: Sustain. Energy Technol. Assessments, vol. 46, 2021, https://doi.org/10.1016/j.seta.2021.101248.
[48] M.E. Zayed, J. Zhao, W. Li, S. Sadek, and, A.H. Elsheikh, Chapter three - Applications of artificial neural networks in concentrating solar power systems, in: A.H. Elsheikh, M.E. Abd Elaziz (Eds.), Academic Press, 2022, pp. 45–67.
[49] L.D.O. Santos, P.C.M. De Carvalho, and, C.D.O.C. Filho, Photovoltaic cell operating temperature models: a review of correlations and parameters, IEEE J. Photovoltaics vol. 12 (1) (2022) 179–190, https://doi.org/10.1109/JPHOTOV.2021.3113156.
[50] Y.A. Çengel, A.J. Ghajar. Heat and Mass Transfer: Fundamentals & Applications, fifth ed, McGraw-Hill Education, 2015.
[51] A.K. Azad, S. Parvin, Photovoltaic thermal (PV/T) performance analysis for different flow regimes: a comparative numerical study, Int. J. Thermofluids vol. 18 (2023) 100319, https://doi.org/10.1016/j.ijft.2023.100319.
[52] A. Nahar, M. Hasanuzzaman, and, N.A. Rahim, Numerical and experimental investigation on the performance of a photovoltaic thermal collector with parallel plate flow channel under different operating conditions in Malaysia, Sol. Energy vol. 144 (2017) 517–528, https://doi.org/10.1016/j.solener.2017.01.041.
[53] T. Rajeh, B.H. Al-Kbodi, L. Yang, J. Zhao, M.E. Zayed, A novel oval-shaped coaxial ground heat exchanger for augmenting the performance of ground-coupled heat pumps: Transient heat transfer performance and multi-parameter optimization, J Build Eng. 79 (2023) 107781, https://doi.org/10.1016/j.jobe.2023.107781.
[54] I. Dincer, Thermodynamics: A Smart Approach, First, Wiley, 2020.
[55] M. Abd Elaziz, S. Senthilraja, M.E. Zayed, A.H. Elsheikh, R.R. Mostafa, and, S. Lu, A new random vector functional link integrated with mayfly optimization algorithm for performance prediction of solar photovoltaic thermal collector combined with electrolytic hydrogen production system, Appl. Therm. Eng. vol. 193 (2021) 117055, https://doi.org/10.1016/j.applthermaleng.2021.117055.
[56] A. Buonomano, F. Calise, A. Palombo, and, M. Vicidomini, Adsorption chiller operation by recovering low-temperature heat from building integrated photovoltaic thermal collectors: Modelling and simulation, Energy Convers. Manag. vol. 149 (2017) 1019–1036, https://doi.org/10.1016/j.enconman.2017.05.005.
[57] A. Buonomano, F. Calise, M.D. d'Accadia, M. Vicidomini, A hybrid renewable system based on wind and solar energy coupled with an electrical storage: dynamic simulation and economic assessment, Energy vol. 155 (2018) 174–189, https://doi.org/10.1016/j.energy.2018.05.006.
[58] I. AL-Arfi, et al., Thermo-economic and design analysis of a solar thermal power combined with anaerobic biogas for the air gap membrane distillation process, Energy Convers. Manag. vol. 257 (2022) 115407, https://doi.org/10.1016/j.enconman.2022.115407.
[59] M.A. Mellal, 2022, Applications of Nature-inspired Computing in Renewable Energy Systems vol. i.
[60] M. Mitchell, An introduction to genetic algorithms, An Introd. to Genet. Algorithms vol. 24 (2020) 293–315, https://doi.org/10.7551/mitpress/3927.001.0001.
[61] K. Deb, A. Pratap, S. Agarwal, and, T. Meyarivan, A fast and elitist multiobjective genetic algorithm: NSGA-II, IEEE Trans. Evol. Comput. vol. 6 (2) (2002) 182–197, https://doi.org/10.1109/4235.996017.
[62] I.M.R. Najjar, A.M. Sadoun, M. Abd Elaziz, A.W. Abdallah, A. Fathy, A.H. Elsheikh, Predicting kerf quality characteristics in laser cutting of basalt fibers reinforced polymer composites using neural network and chimp optimization, Alex. Eng. J. 61 (2022), 11005-11018, 2022.
[63] E. Kirtepe, A. Güngör, Thermodynamic analysis and experimental investigation of the heat pump photovoltaic/thermal integrated system, Sci. Technol. Built Environ. vol. 27 (9) (2021) 1298–1310, https://doi.org/10.1080/23744731.2021.1927176.
[64] T. Ma, M. Li, and, A. Kazemian, Photovoltaic thermal module and solar thermal collector connected in series to produce electricity and high-grade heat simultaneously, Appl. Energy vol. 261 (2020) 114380, https://doi.org/10.1016/j.apenergy.2019.114380.